Analysis of Foundation Deformations Beneath the Syncrude Tailings Dyke

J. ALENCAR[1], N.R. MORGENSTERN[2] AND D.H. CHAN[2]

[1] Federal University of Para
Para, Brazil

[2] Department of Civil Engineering
The University of Alberta
Edmonton, AB CANADA T6G 2G7
Telephone: 403-492-2176 Fax: 403-492-8198

Submitted to the

Canadian Geotechnical Journal

March, 1994

Analysis of Foundation Deformations Beneath the Syncrude Tailings Dyke

J. ALENCAR, N.R. MORGENSTERN, AND D. H. CHAN

Abstract

The paper presents the results obtained in the finite element simulation of 8 years of construction of a section of Syncrude's tailings dyke, which is located in northern Alberta and has been used to store oil sand mining waste.

The site investigation for the construction of this dyke indicated that a region of the foundation contained a pre-sheared over-consolidated clay-shale lying practically horizontal at about 20 m depth. Significant horizontal displacements have occurred along this layer. The section analyzed in this work is the one which showed the largest horizontal movements in the foundation. High pore pressures have been measured along this section and the lateral displacements measured in the foundation have reached values over 25 cm.

The major purposes of the finite element analyses were to identify the factors which have significantly influenced the deformation mechanisms and to determine a combination of parameters, within the acceptable range of values for each material, that would reproduce satisfactorily the field observations. Linear, non-linear and effective stresses analyses were carried out.

The total stress analyses underestimated the displacements measured in the field very significantly. The displacements calculated by the effective stress analyses are in very good agreement with the measured values and the combination of parameters necessary to reach those results are within the acceptable range of variability for each material involved, based on laboratory test results.

The interpolation of the pore pressures based on the piezometer measurements and their incorporation into the analyses as known quantities at each stage of the loading process was found to be relatively simple and efficient, causing a substantial improvement of the results compared with the total stress analyses.

Keywords: Tailing Dyke, Deformation Analysis, Shear Zone, Effective Stress Modelling, History Matching.

Introduction

Tailings dykes are usually located close to where wastes are generated in order to minimize the cost of waste management. The size of the dyke varies with the scale of the project and in some cases, the aerial extent can be substantial. Since the available space is usually limited, tailings dams may have to be constructed over unfavorable ground conditions.

The surface mining operation to recover bitumen from the Athabasca oil sands at Syncrude Canada Ltd. in Fort McMurray, Alberta, requires the construction of a tailings dyke approximately 24 km in length and over 50 m in height. The dyke is constructed using the tailings sand from the bitumen extraction process and is used to retain a tailings pond. Information about the capacity, dimensions and layout of the dyke has been presented by Handford and Fair (1986).

Site investigation for the construction of the Syncrude tailings dyke indicated a presheared over-consolidated clay shale layer lying practically horizontal at about 20 m depth beneath parts of the foundation. Significant amounts of movement were observed during construction of the dyke along this weak presheared layer. The largest foundation movement recorded up to 1986 had exceeded 25 cm (Fair and Handford, 1986) at Section 53, Cell 23. Pizeometric measurements showed substantial increases in pore pressure during construction. Due to the slow rate of construction of the dyke and careful monitoring of extensive instrumentation, the design of the dyke was based on observational methods. The application of the observational method is familiar to geotechnical engineers (Peck, 1969). In this approach, the design is modified based on the observed performance of the structure. Changes in subsequent design of the structure is usually based on local or previous experience with similar situations. The practical application of the method is therefore largely empirical.

With the rapid advent of computer methods in many fields of engineering, the process of obtaining a solution for a deformation problem has become much simpler. Numerical methods, such as the finite element method, are often perceived as a tool to make predictions of deformation for use in design. This may be the case when the material behaviour, properties and boundary conditions can be determined with sufficient accuracy. However, this is not practical for many geotechnical problems. The complexity of material response and the difficulties associated with determining the subsurface conditions accurately make it very difficult, if not impossible, to make a so-called Class A prediction

with confidence. Understanding these inherent uncertainties in a geotechnical problem has lead the authors to advocate the integration of numerical analysis with the observational method in order to improve design in an on-going manner (Chen et al, 1992).

In analyzing a geotechnical structure which involves stage construction, the prior observed performance of the structure can be used as a basis for fine tuning the numerical model for use in predicting subsequent movements of the structure. Of course, it is necessary to first construct a model which reasonably represents the condition of the site and the anticipated response of the material. The predicted deformation of the structure may deviate from the early observed response. The history-matching of the model based on field performance implicitly accounts for some of the unknowns, such as subtle variations in material properties, which may not have been explicitly built into the numerical model. This not only helps in making improvements to the numerical model, but it also aids the application of the observational method by providing more specific insight into the behaviour of the structure. Numerical modelling facilitates the integration of all observations in performance assessment.

This paper presents the results of a finite element simulation of 8 years of construction of a section of the Syncrude tailings dyke; Cell 23 section 53+00E. The purpose of the analysis is to identify the factors which significantly affect the deformation behaviour of the dyke and to obtain a combination of the controlling parameters, within an acceptable range of values, which could satisfactorily reproduce the field observations. Previous works related to other dam construction pursuing similar objectives have been reported in the literature, e.g. Morgenstern and Simmons(1982). Most analyses, so far, have been performed in terms of total stresses to avoid difficulties associated with explicit incorporation of pore pressure changes during construction into the numerical model. These total stress procedures, when applied to cases where pore pressure changes are significant, require the determination of equivalent total stress parameters to match the observed behaviour. Since the total stress parameters are sensitive to changes in pore pressure, it is therefore difficult to determine a set of parameters for use in analyses. The effective stress approach, which is adopted in the present study, provides a better framework for the solution of a geotechnical problem.

Geology of the Site and Soil Stratigraphy

The Syncrude Canada Ltd. operation is located in Fort McMurray, Alberta. Bitumen is recovered from the Athabasca oil sands by surface mining and processing through an extraction plant. Tailings sand is produced and transported using pipelines to construct a 24 km dyke surrounding the tailings pond.

The geology at the site where the tailings dyke is constructed has been described by Fair and Handford(1986). The stratigraphic sequence for the specific section being analyzed in the present work, Cell 23 Section 53, is shown in Figure 1. The subsurface conditions consist of an upper layer of fluvial dense sand (designated as pf) with an average thickness of 4 m, underlain by a layer of stiff sandy silt till (pgs) whose thickness increases from 3 m close to the center of the dam, to 10m close to the toe. In the region near the center line below the sandy silt till, there exists an 8 m thick layer of stiff clayey till (pgc), which ends at approximately halfway between the center line and the toe. Below the clayey till are the basal units of clay shale of the Clearwater Formation.

The top unit of the Clearwater Formation, referred to as kca, is a 5 m thick dark slickensided dark grey clayey-silt, thinly laminated with churned bedding. The layer underneath the kca material, referred to as kcw, is a grey colored and fissured clay shale approximately 2 m thick. Substantial amounts of movement have been observed in the kcw material during the construction of the dyke. The oil sand of the McMurray Formation is found underneath the kcw material. It is bitumen rich and is in a very dense interlocked state which exhibits high strength and stiffness.

Shear Strength Properties of the Foundation Materials

Triaxial and direct shear tests were carried out to determine the deformation and shear strength properties of the foundation materials and the compacted tailings sand. A series of undrained and drained triaxial extensions tests were conducted at the University of Alberta on the sandy till (pgs) samples obtained from Cell 23, Section 50, using a pitcher sampler. Syncrude Canada also performed direct shear tests on intact and slickensided samples of the clayshale (kcw) material. The shear strength parameters thought operational at the time are summarized in Table 1.

Dyke Construction, Construction Monitoring and Performance of the Dyke

The downstream slope of the dyke was originally designed with a slope of 4:1 (four horizontal to one vertical). However localized movements along the kca/kcw contact were observed since 1981. By the end of 1983 it was decided that the downstream slope should be flattened to 8.5:1 resulting in an overall slope of approximately 6.8:1. The new slope configuration was based on limit equilibrium analyses which indicated that the factor of safety at the ultimate height of the dyke, crest elevation 352 m, would be increased from 1.09 to 1.33 with the new inclination. The construction sequence is shown schematically in Figure 1.

Summary of the field instrumentation installed in Cell 23 has been presented by Fair and Handford(1986). Therefore it suffices only to provide a brief description of the instrumentation results of Section 53 which are relevant to the present work.

Slope Indicators

A plan view of the slope indicator locations at Section 53 is shown in Figure 2 and a cross section in Figure 3. The first slope indicator installed was SI 81-23-02, in the spring of 1981, at Berm 319. This slope indicator indicated horizontal movement of approximately 3 cm that year. Slope indicator SI 81-23-03 was installed at the toe of Section 53 in 1981. By the end of 1983 SI 81-23-02 indicated an additional 5 cm of horizontal movement, while at the toe 3 cm of movement was registered. In July 1984 slope indicator SI 84-23-31 was installed at approximately 55 m from SI 81-23-02 towards the center of the dam (see Figures 2 and 3).

Each slope indicator was used to measure movements of the dyke until the horizontal displacement over a 60 cm length reached approximately 5 cm. At this point another slope indicator was installed close to its location and additional movements were added to the latest installed slope indicator. Hence in Figure 2 there is more than one instrument at the same location.

By the end of 1984 a total horizontal displacement of 15.5 cm was registered at elevation approximately 290 m, close to the kca/kcw interface at the location of SI842332. At the same elevation, 4.5 cm of horizontal movement was recorded at SI842331. The region where the largest horizontal movements were observed is called the shear zone or the critical region. At the toe of the dyke movement of approximately 3.8 cm was

recorded. In April 1985 slope indicator SI852325 was installed in Section 53. By the end of 1985, at an elevation close to the kca/kcw interface, the horizontal displacement recorded at slope indicator SI842334 had reached approximately 9.0 cm, almost 22 cm at slope indicator SI842332 and 8.0 cm at the toe. By the end of 1986 these values had increased to, approximately, 11 cm, 26 cm and 10 cm respectively. Slope indicator measurements showed that there is very little deformation in the till material above the clay shale and therefore there is very little shear straining in the pgs material.

In the design of major earth structures, it is common practice to use a high factor of safety to control the amount of deformation. For the case of Cell 23 of the Syncrude Tailing dyke, the factor of safety of the dyke in 1986 was calculated to be 1.6. Despite such a high factor of safety, lateral movement was extremely sensitive to dyke construction. This illustrates the importance of combining the observational approach with advanced deformation analysis in this class of problems.

Sliding micrometers

Sliding micrometers are instruments which measure the axial strain distribution along a borehole (Kovari and Amstad, 1983). Description of the equipment installed at the Syncrude tailings dyke as well as the calibration procedure, problems encountered during installation and measurements obtained have been presented by Handford and Fair (1986). Two inclined sliding micrometers were placed in Section 53, one at the toe and the other at approximately 60 m downstream from the toe, at inclinations of 23° and 13° below horizontal and lengths of 36 and 53 m, respectively, see Figure 3. A third unit was installed vertically at the toe, but the application was limited as the occurrence of small horizontal slips were impossible to distinguish from extension due to heave (Handford and Fair, 1986).

An initial set of readings were taken before 1985. The micrometers TSMA3 located at the toe of the dyke and TSMA5, downstream from the toe, showed average axial compressive strains in the pgs material of 0.2 and 0.44 mm/m, respectively. TSMA3 showed practically no axial straining in the pf sand layer. Both instruments indicated extensional spikes at the region where the horizontal slip was observed. Generally, the average strains measured by the sliding micrometers are consistent with the average strain determined from adjacent inclinometers.

Piezometers

A plan view of the pneumatic piezometers installed in Section 53 is shown in Figure 4 and a cross section is given in Figure 5. There were relatively few piezometers before 1983. Additional piezometers were installed in 1983 when the downstream slope was flattened.

There was a substantial increase in pore pressures in the region close to the kca/kcw interface due to the construction of the dyke. This is illustrated in Figure 6 where the average phreatic line in the sand for each year and the piezometric elevations for points close to the kca/kcw interface in 1986 are presented. Pore pressures measured at Piezometers PN852307 and PN852311 are shown in Figure 7, in which this local increase can be clearly observed.

Finite Element Analysis

The construction of the dyke was simulated using a two dimensional finite element model. The finite element mesh, shown in Figure 8, is composed of 391 6-node triangular and 8-node quadrilateral isoparametric elements. The final crest elevation of the dyke is equal to 352m which was expected to be reached in 1993. The present analysis involves the construction period between 1979 and 1986. Figure 1 shows the construction stages from 1979 to 1986.

Figure 8 illustrates the soil stratigraphy in the finite element model. Linear and nonlinear elastic and plastic models were used to describe the deformation response of the materials. The analysis was carried out using the finite element program PISA (Program for Incremental Stress Analysis) developed at the University of Alberta (Chan 1986). This program is capable of performing one, two and three dimensional linear and non-linear elastic as well as elastic-plastic analyses involving various yield criteria. The analyses can be performed in terms of total or effective stresses (Chan and Morgenstern, 1992).

The finite element simulation was carried out in two stages. The first stage was the incorporation of the initial stress field in the foundation material. The exact magnitudes of the stresses at every point are not known but it is believed that the coefficient of earth pressure at rest (K_o) is around 0.8 to 1.0 at Section 53, to reflect glacial drag processes. The initial stress field was applied using a "switch-on-gravity" technique. The vertical

stresses generated due to the application of the gravity forces are close to the total weight of the material above a given point and the horizontal stresses are dependent on the Poisson's ratio, ν, of the material. For a homogeneous isotropic linear elastic material under no lateral movement the K_o value is equal to $\nu /(1- \nu)$.

Following the switch-on-gravity stage, the construction of the dyke was carried out in a number of steps. Each step represents the construction of one layer of material. The thickness of each layer in the finite element model corresponds to the material placed in one construction season, see Figure 1.

Different types of analyses were performed in this study. They include linear elastic analysis, total stress non-linear analysis and effective stress non-linear analysis. Although the material behaviour is expected to be non-linear and governed by effective stresses, linear elastic analysis provides considerable insight into the problem by providing a basis for comparison with non-linear analysis. Since linear analysis requires no iterative process in obtaining a solution, it is easy to perform. Non-linear total stress provides an increased level of sophistication in the modelling, but avoids the effect due to pore pressure. The results are of interest for comparison with effective stress non-linear analyses.

Linear Elastic Analysis

A number of elastic analyses were performed and the elastic parameters are summarized in Table 2 (De Alencar, 1988). Figure 9 shows the calculated horizontal movement of slope indicator SI842332 from the finite element analysis. Different elastic moduli were used for the till and the clay shale materials in order to examine the effect of the modulus on the deformation behaviour of the foundation. The results suggest that in order to model the localized slip along the kca/kcw interface, varying the moduli of the pgs, pgc or kca materials alone would not lead to the correct mechanism. The deformation pattern can only be achieved by a substantial reduction of the modulus of the kcw material. This does not mean that kcw is a soft material. It means that there is a continuous shear plane, or a number of closely spaced horizontal planes, that have been presheared due to past geological events such as glacial drag. This weak zone may be located in the kca or kcw materials or at their interface. It is therefore convenient in the finite element model to model this shear plane using the kcw material.

The Figure shows results for a case in which the kcw elastic modulus was drastically reduced. In the same figure the field measurements obtained until the end of 1985 are plotted for comparison. Even though the lateral movements above the km material are underestimated, it is observed that the elastic model does develop a distinct localization of movements along kcw material. The observed localization of movements at elevation 290 m can only be modelled by allowing slip to take place in the kcw material.

Material Models for the Non-linear Analysis

The material models and parameters used in the total stress analyses are summarized in Table 3. Due to the small amount of movement observed in the McMurray oil sand, km material, a linear elastic model is adopted for this material. Results from the linear analysis suggested that in order to match the finite element model with the observed deformation mechanism, the shearing resistance of the kcw material should be relatively low. This is consistent with observations on samples. Therefore, an elastic perfectly plastic model with a Mohr-Coulomb yield criterion is used for this material. The kca material is dark, slickensided with thinly laminated grey clay silt and is believed to have been presheared. The Mohr-Coulomb elasto plastic model is also used for this material.

Triaxial tests were carried out to determine the stress-strain characteristic of the till material, pgs and pgc materials. The results showed that the stress-strain relationship can be approximated by the hyperbolic model proposed by Duncan and Chang (1970) up to an axial strain of about 2 %. It is estimated, based on the slope indicator measurements, that the amount of straining in the till material is around 0.2 %. Therefore the nonlinear elastic hyperbolic model should be a reasonable model for these materials. The hyperbolic model was also used for the fluvial sand (pf) and the tailings.

Total Stress Analysis

Several total stress analyses were carried out. In these analyses a sensitivity study was carried out in which the material parameters were varied, within a reasonable range based on the results of the triaxial test, in order to examine their effects on the deformation behaviour of the foundation. It is also of interest to look for a combination of parameters that would yield a model which would closely match the observed field measurements. In

all of the analyses the loading process was modelled by successive placement of soil layers. Each corresponds to one year of construction of the dyke. These layers were initially placed as linear elastic materials with a low modulus of deformation representing the placement process. When the overlying layers were placed in subsequent steps, the material was changed to the hyperbolic model. This technique was used to avoid the problem of zero initial stress in the hyperbolic model. When the material was initially being placed, the confining stress would be very low, close to zero at the surface, which would result in a very low or zero modulus. A zero modulus will cause numerical problems. Therefore an elastic model was used with a non-zero modulus.

Table 3 shows the material parameters used in analyses NLT-1 to NLT-7. The simulation was carried out up to 1985. In cases where the combinations of material parameters led to numerical instability, or gave results very similar to previous combinations, the analysis was terminated before reaching the final height of the dyke.

Analysis NLT-1 - Initial Analysis

This analysis was based on assumed soil properties for the pgc and pgs materials before triaxial test results were available. Friction angles close to residual values were used for kca and kcw materials assuming presheared conditions for these materials. The calculated horizontal displacements at inclinometers SI842334 and SI842332 are compared with field measurements as shown in Figures 10 and 11. It should be noted that the slope indicators were not installed at the beginning of the dyke construction. Therefore some displacements had already occurred in the dyke which could not be recorded by the inclinometers. When comparing the calculated displacements with the observations, the total calculated displacements were subtracted from the displacements at the time when the inclinometers were installed. This correction was applied in all calculated slope indicator movements when comparing with field measurements. The finite element model has underpredicted the movement at both slope indicator locations. It seems that the pgs and pgc materials were too stiff.

Analysis NLT-2 - Reduce modulus of pgc material

Realizing that the modulus of the pgc material was probably too high, its value was therefore reduced by about 65% keeping all other parameters unchanged. The calculated horizontal displacements, also shown in Figures 12 and 13 indicate no significant

differences in displacements in comparison with previous analysis NLT-1. It should be noted that pgc is in the active zone and does not contribute much to the restraining mechanism.

Analysis NLT-3 - Reducing frictional angles of kca and kcw materials

Reduction of the friction angles for the kca and kcw materials was considered, since the results of the linear elastic analysis showed that the existence of a continuous low strength material was necessary in capturing localized slipping. In this analysis the total stress friction angles of the kcw and kca materials were reduced to 4°. Direct shear tests performed in kca and kca/kcw transition suggested an average residual effective stress angle of around 8°. However in a total stress analysis, the generation of pore pressure in the material can reduce the total stress friction angle to below the effective stress friction angle. Therefore, an angle of 4° would reflect the reduction of shear strength due to an increase in pore pressures during shear deformation.

The results are also compared to field measurements in Figures 10 and 11. It is seen that at SI842332, the finite element model shows localized slipping although the amount of slip is underestimated compared to field measurements. No slipping has occurred at SI842334 although the amount of movement at this location is greater than previous analysis.

Analysis NLT-5 - Reducing elastic modulus of kca and kcw materials

To examine the effect of changing the elastic moduli of the kca and kcw materials, the moduli were reduced to 200 MPa. Figures 12 and 13 show a slight increase in movements at the critical region. It is therefore evident that the strength properties have more effect on the localized movements than the deformation properties of these materials. Since the strength properties control the extent of yielding of the material and the stiffness of the material changes considerably after passing the peak strength, the amount of movement is more sensitive to the strength of the material.

Analysis NLT-6 - Reduce frictional angle of pgs material

In this analysis the internal friction angle of the pgs material was reduced to 16° with a cohesion intercept of 50 kPa. The laboratory test results indicated that the total stress friction angle for pgs material is around 16-17°, and the cohesion intercept may vary from 0 to 150 kPa depending on the amount of straining in the soil. The decrease in the strength of the pgs material results in an increase in horizontal movements in the kcw, kca and pgs materials as shown in Figure 13. However the calculated displacement is still less than the observed values in the critical region.

Analysis NLT-7 - Increase Poisson's ratio of the kcw material

During the construction of the dyke, high pore pressure was observed in the kca/kcw materials. This indicates that the material was deforming closer to an undrained condition than a drained condition. To model undrained deformation in total stress analysis, the Poisson's ratio of the material should be set close to 0.5. A Poisson's ratios of 0.5 can result in an incompressible material with infinite bulk modulus which can cause numerical problems. Therefore a Poisson's ratio of 0.47 was used in this case.

The results of the analysis are presented in Figures 12 and 13. Comparing the calculated and observed displacements, it is seen that not only has the finite element model underestimated the observed movements, the shape of the displacement curves are quite different. The field curves show very little distortion in the pgs material, especially beneath Berm 319, giving the impression of a rigid block movement, while the calculated curves show a larger amount of distortion in kca and pgs.

During the initial loading stages the shear stresses in the clay shale, kca and kcw materials, were not high enough to cause substantial movements in these materials. As loading was increased due to additional fill placement, localized yielding was induced in the kca and kcw materials. Since these materials are weaker than the overlying till, the horizontal displacements along those layers tended to be greater than in the till material. This leads to a change in the mechanism of deformation from generalized straining in the till to slip along the weak clay shale layers. Once the shearing resistance in the weak clay shale material has been mobilized, additional loading due to dyke construction can only be resisted by the till material which provides a strutting effect against overall failure of the dyke. This mechanism of deformation is consistent with the observed deflected shape of the inclinometers.

By inspection of the NLT-7 analysis it was observed that an increase in the Poisson's ratios for the kcw and kca materials leads to a rotation of the principal stresses at the toe of the dyke. This rotation of the principal stresses results in higher horizontal stress in the till, and consequently, higher horizontal displacements result. Figure 14 compares the measured and calculated displacements at the elevation corresponding to the kca/kcw interface at inclinometer SI842332. It is seen that the finite element model overestimates the displacements up to 1982 but underestimates the displacements after that.

The non-linear total stress analyses demonstrated that the movements are very much dependent on the strength and deformability parameters of kca, kcw and pgs materials. The analyses provide a better understanding of the changes in the deformation mechanisms that developed during construction of the dyke and help to explain the observed shape of the inclinometer measurements. The calculated displacement curves, although underestimating the field values, are in reasonable agreement with the observed shapes.

Since the total stress approach accounts for the effect of pore pressure in an implicit manner, the effect of pore pressure variations cannot be taken into account in the analysis. The material parameters determined in the laboratory do not necessary provide the best values in capturing the behaviour observed due to large differences in stress paths and pore pressure generation in the field. Therefore proper modelling of the deformation of the dyke can only be carried out in terms of effective stress.

Effective Stress Analysis

In carrying out an effective stress analysis, it is necessary to calculate the pore pressure in the soil for the entire domain. There are many ways of calculating pore pressure in the soil. One approach is to couple the deformation of the soil with the generation and dissipation of pore pressure. This requires the determination of the consolidation and seepage characteristics of the materials. Accurate predictions of pore pressure are often difficult due to difficulties in determining the permeabilities of the soils, in defining the boundary conditions of the problem and in locating macro and micro features, such as fissures and joints, which can significantly affect the flow of water and the rate of consolidation.

A different approach that avoids prediction is to prescribe pore pressure in the soil provided that pore pressure measurements are available. In the present analysis, pore

pressures have been monitored at Section 53 for a considerable amount of time and detailed information is available. Therefore it is prudent and more effective to incorporate the observed pore pressure rather than rely on predicted pore pressure in the effective stress analysis. The method of incorporating measured pore pressure in a finite element analysis can be found in De Alencar et. al., 1992 and De Alencar, 1988.

As in the total stress analyses, the material parameters were varied to examine their effect on the behaviour of the structure.

Pore Pressures

At Section 53 pore pressures were observed in the foundation and dyke at several locations and depths. The pore pressure measurements are very localized. In order to perform an effective stress analysis, it is necessary to determine pore pressure for the entire domain. An interpolation scheme is used to interpolate the pore pressure from the piezometric locations to every point in the domain, as per De Alencar et. al. 1992.

The initial pore pressure distribution in the foundation before the construction of the dyke was assumed to be hydrostatic with the phreatic surface at elevation 300 m. After each lift the phreatic surface was raised as shown in Figure 7. Pore pressures were assumed to be hydrostatic for points below the phreatic surface, i.e., their values were calculated as the vertical distance between the point being considered and the phreatic line multiplied by the unit weight of the water. Obviously, this is not in accordance with the measured values where a substantial localized increase was observed close to the kca/kcw interface elevation. The initial assumption of pore pressure distribution for each year was then corrected as a function of the average field pore pressure measurement at that year. The initial and corrected values are compared to the field measurements along piezometers PN852307 and PN852311 as shown in Figures 15 and 16 respectively.

Analysis NLE-1

The material parameters used in the analysis are summarized in Table 4. These values are based on triaxial testing of the pgs and pgc materials. The friction angle for the kcw material was set equal to the average residual value of 8° and the friction angle for the kca material was set approximately equal to the peak value of 14° for the slickensided

samples on direct shear tests. The initial water level was considered to be at elevation 300 m.

The calculated displacements were found to be too small at the critical region when compared with the observed measurements. Therefore the analysis was terminated early in 1982. At that stage the calculated horizontal displacement at SI842332 location at the kca/kcw interface was 1.9 cm, while the observed measurement was approximately 3 cm. Other analyses carried out, but not reported here, indicated that the final displacements in 1986 will be underpredicted.

Analysis NLE-2

To increase the amount of slip at the shear zone and explore sensitivity to properties, the cohesion intercept of the pgs material was reduced to zero and the friction angle was increased to 38°. This results in no significant changes in the displacements along kca/kcw interface relative to previous calculations. This is due to the fact that the amount of movement at the shear zone is dependent on the stiffness of the overlying layer and the strength properties of the shear zone. By reducing the cohesion of the overlying material, the deformation modulus was not significantly affected and therefore the amount of movement remains unchanged. Varying the shearing resistance of the shear zone will have a larger effect on the movement of the foundation.

Analysis NLE-3

In this analysis the friction angle of the kca material was reduced to 11° and the friction angle of the kcw material to 7.5°. The displacements were increased with respect to previous analyses but were still too small. At SI842332 location, the calculated horizontal displacement at the kca/kcw interface was 2.1 cm in 1982, while the measured displacement was 3 cm. In 1983 the difference between the calculated and measured values increased to 4.2 cm. Based on the laboratory tests results and limit analysis of the dyke at other locations, it is believed that the friction angle of the kca and kcw should not be lower than 11° and 7° respectively.

Analysis NLE-4

To examine the effect of varying pore pressures on the amount of movement, the initial water table in the till layer was increased from elevation 300 to 305 m. In this case the calculated displacements at kca/kcw interface at SI842332 position were closer to the measured values up to 1982, but the discrepancy increased significantly after 1983.

The effect of increasing the initial water level was a lower confining effective stress at the early stages of loading. This reduces the stiffness of the till material and results in larger movements.

Analysis NLE-5

The initial water level in the till was raised to the ground surface. The friction angle of the kcw and kca materials were increased slightly to 8° and 14° respectively in order to reduce the movements in the initial load stages. It is recalled that 8° corresponds approximately to the residual strength for the kcw material, while 14° corresponds to the shear strength of the slickensided kca material.

The results of this analysis are in much better agreement than any of the previous analyses up to the 1983 load stage. However, when the loading for 1984 was applied, tension developed in the kcw materials close to the toe of the dyke. The program PISA handled tension using the stress transfer technique (Zienkiewicz et al, 1968). In this method the tensile stresses in the affected elements are eliminated by the application of a fictitious load. Due to the stiffness of the elements, the application of the fictitious load will generate some tensile stresses. The process is repeated until all tensile stresses are removed. The rate of convergence is usually very slow. In order to improve the efficiency in relieving tension, an anisotropic no tension model was implemented in PISA, Chen and Suzuki (1980) and De Alencar (1988). The new scheme assumes the element is cracked perpendicular to the direction of the tensile stress. The stiffness across the cracks is reduced to zero and the stiffness in the orthogonal direction is maintained thus resulting in a biaxial stress condition.

The use of the cracking model improved numerical stability and enabled the analysis to be continued. The results for the years 1985 and 1986 are compared to the field measurements in Figures 17 to 19. It is observed that the shapes of the curves as well as the values of the displacements are in better agreement with the field values. It should be

pointed out that the friction angle for the kcw material is more realistic than in the total stress analysis.

It is seen in Figure 17 that the shape of the calculated displacement curves at SI842334 are in reasonable agreement with the observations. In 1985, the field values were underestimated by about 35%, but in 1986 this percentage dropped to less than 10%. Beneath Berm 319, see Figure 18, very good agreement is obtained between measured and calculated displacements. The calculated displacements in 1985 and 1986 represent, approximately, 75% and 90% of the measured values, respectively. At the toe, the calculated values of displacements are very close to the field measurements, as shown in Figure 20. In 1986 an almost perfect match is obtained.

Comparison between calculated and measured displacements at the kca/kcw interface in Berm 319 and toe at different times is shown in Figure 21. It is observed that in both locations the calculated values show the same trend as the field data. Beneath Berm 319 a slight overestimation of the movements before 1983 has occurred and an underestimation after that is found. In the case of the displacements at the toe the differences between calculated and measured displacements are much smaller. The horizontal displacements along an approximately horizontal plane corresponding to the kca/kcw interface is shown in Figure 21. The locations of three slope indicators are presented for a clearer interpretation of the figure, but no comparison between measured and calculated values is shown since, in this case, the total displacements are plotted, i.e., they were not subtracted from the amount of displacement calculated for the period of time before the installation of the slope indicators. Figure 21 shows, in accordance with what has been observed in the field, that the higher displacements occur beneath the berm 319 region and decrease rapidly towards the toe and the center of the dam.

Contours of maximum shear strains are shown in Figure 22 for the year 1986. It is noted that a zone of high distortion is concentrated in a region adjacent to the kca/kcw contact. Very little distortion is observed in the pgs material, which is in agreement with the movement pattern given by the slope indicator measurements in the field. With respect to extensional strains, the cracking model indicated in 1984 the formation of practically vertical superficial cracks close to the position of SI842334 and 2 cracks with orientations of approximately 30° clockwise relative to the horizontal in kcw material at the toe. These cracks express a movement pattern with a descending horizontal sliding close to SI842334 and upwards inclined movement close to the toe.

In 1985 the computed vertical cracks deepened and more cracks appeared in the kcw material at the toe. The results may be considered to agree with the micrometer measurements at the toe, which presented an overall compressive state, except at the kca/kcw interface region. However, it is not possible to decide whether the measured extensional strains were real or due to the horizontal sliding. The orientations of the cracks at the end of 1986 are schematically presented in Figure 23.

Conclusions

The analysis of Section 53, Cell 23, of the Syncrude tailing dyke provides valuable experience on the modelling capability for this class of problem which involves complicated geological conditions with presheared weak layers and complicated stage construction procedures with significant foundation movements. The analysis shows that it is possible and effective to construct a numerical model using a history matching approach and that this provides insight for the evaluation of performance. Although the following conclusions are applicable to the present study, they are in general true for the class of problem being examined.

1. The effective stress approach provides a better model than the total stress approach. The explicit account of the pore pressure is important in this problem.

2. When the movement in the foundation of an embankment is localized in presheared weak layers, the pore pressure and the shear strength of the weak layers are very important in determining the amount of movement. The stiffness of the weak layer is of lesser importance once the shear strength of the material has been mobilized.

3. The stiffness of the material above the weak layer in the restraining zone has an important effect on the amount of movement at the weak layer. The shear strength of the overlying material has a lesser direct effect on the movement although the shear strength can affect the stiffness of the material.

4. The incorporation of measured pore pressure into the finite element scheme can be achieved in a relatively simple manner making effective stress analysis more amenable in finite element calculations.

Acknowledgment

The authors wish to acknowledge the support offered by Syncrude Canada Ltd., specially by Mr. Gerry Handford, allowing access to the records relative to the construction of the tailings dyke. The financial support provided by the Brazilian Government through "Coordenacao de Aperfeicoamento de Pessoal de Nivel Superior" (C.A.P.E.S.) for one of the authors to develop his studies is also gratefully acknowledged.

References

Chan, D., 1986. "Finite Element Analysis of Strain Softening Material". Ph.D. Thesis, University of Alberta.

Chan, D. and Morgenstern, N., 1992. "User Manual of Program PISA", The University of Alberta, Edmonton, Alberta.

Chen, Z. and Chan, D., 1993. "Numerical Stability of Strain Weakening Finite element Calculation", International Conference on Soft Soil Engineering, Guangzhou, China, p 80-85.

Chen, W.F. and Suzuki, H., 1980. "Constitutive Models For Concrete". Computers and Structures, Vol. 12, pp. 23-32.

Chen, Z., Morgenstern, N. and Chan, D., 1992. "Analysis of the Carsington Dam - A Numerical Study", Canadian Geotechnical Journal, **29**: No. 6, p 971-988.

De Alencar, J.A., 1988. "Deformation of Dams on Sheared Foundations". Ph.D. Thesis, University of Alberta.

De Alencar, J.A., Chan, D.H. and Morgenstern N.R., 1992. "Incorporation of Measured Pore Pressure in Finite Element Analysis", Proceeding of the 45th Canadian Geotechnical Conference, Toronto, Ontario, Oct. 26-28, p 62-1 - 62-10.

Duncan, J.M. and Chang, C.Y., 1970. "Nonlinear Analysis Of Stress and Strain In Soils". Journal of the Soil Mechanics and Foundations Division, ASCE, Vol. 96, SM 5, pp. 1629-1653.

Fair, A.E. and Handford, G.T., 1986. "Overview of Tailings Dyke Instrumentation Program at Syncrude Canada Ltd.". Proceedings International Symposium on Geotechnical Stability in Surface Mining, Calgary, pp. 245-253.

Handford, G.T. and Fair, A.E., 1986. "In Situ Strain Measurements Using The Sliding Micrometer At Syncrude's Tailings Dyke". Proceedings 39th Canadian Geotechnical Conference, Ottawa, pp. 277-282.

Kovari, K. and Amstad, C., 1983. "Fundamental of Deformation Measurements". Proceedings, International Symposium on Field Measurements in Geomechanics, Zurich, Vol. 1, pp. 219-239.

Morgenstern, N.R. and Simmons, J.V., 1982. "Analysis of the Movements of Gardiner Dam". Proceedings 4th International Conference on Numerical Methods in Geomechanics, Vol. 3, pp. 1003-1027.

Peck, R.B., 1969. "Advantages and Limitations of the Observational Method In Applied Soil Mechanics". Geotechnique, Vol. 19, pp. 171-187.

Zienkiewicz, O.C., Villiappan, S. and King, A.P, 1968. "Stress Analysis of Rock as a 'No Tension' Material". Geotechnique, Vol. 18, pp. 56-66.

TABLE 1: Summary of Shear Strength Parameters

Material		Peak		Residual	
Name	Sym	c'_p (kPa)	ϕ'_p	c'_r (kPa)	ϕ'_r
Tailing Sand	ts	33	38°	20	30°
Sandy Till	pgs	20-30	30°-37°	20-30	20°-37°
Clayey Till	pgc	11	32°	11	32°
Clayshale	kcw	0	23°	0	7.5°
Clayshale	kca				
Intact		0	23°	0	7.5°
Slickenside		0	12.5°	0	7.3°

MATERIAL																
MAT.	km		kcw		kca		pgs		pgc		pf		ho		ts	
Weight	21.5		20.0		20.0		21.5		21.5		20.0		20.0		20.0	
LE#	E	u	E	u	E	u	E	u	E	u	E	u	E	u	E	u
1	200000	0.45	70	0.30	50	0.45	100	0.40	100	0.40	70	0.30	70	0.30	70	0.30
2	200000	0.45	70	0.30	50	0.45	100	0.40	100	0.40	70	0.30	70	0.30	70	0.30
3A	200000	0.45	70	0.30	50	0.45	50	0.40	50	0.40	70	0.30	70	0.30	70	0.30
3B	200000	0.45	70	0.30	50	0.45	150	0.40	150	0.40	70	0.30	70	0.30	70	0.30
4A	200000	0.45	70	0.30	25	0.45	100	0.40	100	0.40	70	0.30	70	0.30	70	0.30
4B	200000	0.45	70	0.30	75	0.45	100	0.40	100	0.40	70	0.30	70	0.30	70	0.30
5	200000	0.45	5	0.30	50	0.45	100	0.40	100	0.40	70	0.30	70	0.30	70	0.30

Notes:

E - Elastic modulus (MPa)
u - Poisson's ratio
Weight - Unit Weight (kN/m^3)
ts - Tailing sand

Table 2: Summary of material parameters in the linear elastic analyses

Parameters used in the total stress analyses										
Anl.	Par.	Km	Kcw	Kca	Pgc	Pgs	Pf	Ts1	Ts2	Ts3
	E	2000	45	45	-	-	-	5	-	
	u	0.35	0.45	0.45	0.40	0.40	0.30	0.30	0.30	
	ϕ		8.00	8.00	38.70	37.00	38.00		38.00	
1	c				35.00		35.00		35.00	
	k				750.00	410.00	280.00		750.00	
	n				0.24	0.69	0.65		0.24	
	Rf				0.87	0.9	0.93		0.87	
	E	2000	45	45				5		
	u	0.35	0.45	0.45	0.40	0.40	0.30	0.30	0.30	
	ϕ		8.00	8.00	38.70	37.00	38.00		38.00	
2	c				5.00		35.00		35.00	
	k				250.00	410.00	280.00		750.00	
	n				0.24	0.69	0.65		0.24	
	Rf				0.87	0.90	0.93		0.87	
	E	2000	45	45				5		10
	u	0.35	0.45	0.45	0.42	0.30	0.30	0.30	0.30	0.30
	ϕ		4.00	4.00	30.00	38.00	30.00		38.00	
3	c				5.00		5.00		35.00	
	k				150.00	400.00	280.00		750.00	
	n				0.24	0.50	0.50		0.24	
	Rf				0.87	0.90	0.93		0.87	
	E	2000	45	45				5		10
	u	0.35	0.45	0.45	0.42	0.30	0.30	0.30	0.30	0.30
	ϕ		4.00	14.00	30.00	37.00	30.00		38.00	
4	c				5.00		5.00		35.00	
	k				150.00	400.00	280.00		750.00	
	n				0.24	0.50	0.50		0.24	
	Rf				0.87	0.90	0.93		0.87	
	E	2000	20	20				5		10
	u	0.35	0.45	0.40	0.42	0.30	0.30	0.30	0.30	0.30
	ϕ		4.00	14.00	30.00	37.00	30.00		38.00	
5	c				5.00		5.00		35.00	
	k				150.00	400.00	280.00		750.00	
	n				0.24	0.50	0.50		0.24	
	Rf				0.87	0.90	0.93		0.87	

	E	2000	20	20				5		10
	u	0.35	0.45	0.40	0.42	0.30	0.30	0.30	0.30	0.30
	ϕ		4.00	14.00	30.00	16.00	30.00		38.00	
6	c				5.00	50.00	5.00		35.00	
	k				150.00	400.00	280.00		750.00	
	n				0.24	0.50	0.50		0.24	
	Rf				0.87	0.90	0.93		0.87	
	E	2000	20	20				5		10
	u	0.35	0.47	0.47	0.45	0.40	0.40	0.30	0.30	0.30
	ϕ		4.00	14.00	30.00	25.00	30.00		38.00	
7	c				5.00	100.00	5.00		35.00	
	k				150.00	400.00	280.00		750.00	
	n				0.24	0.50	0.25		0.24	
	Rf				0.87	0.90	0.93		0.87	

E - Elastic Modulus (Mpa)
u - Poisson's Ratio
ϕ - Friction Angle (degree)
c - Cohesion (Kpa)
k - Modulus number for hyp. model
Rf - Failure ratio for the hyp. model
Unit weights same as Table 2

Ts1 - Tailing sand using linear elastic model when layer is added
Ts2 - Tailing sand using linear elastic model
Ts3 - Tailing sand using linear elastic model to miminize convergence problem at the toe of the dyke

Table 3: Summary of the material parameters used in the non-linear total stress analyses

Parameters used in the effective stress analyses										
Anl.	Par.	Km	Kcw	Kca	Pgc	Pgs	Pf	Ts1	Ts2	Ts3
	E	2000	45	45	-	-	-	5	-	10
	u	0.35	0.45	0.45	0.40	0.40	0.30	0.30	0.30	0.30
	ϕ		8.00	14.00	11.00	25.00	35.00		35.00	
1	c				32.00	33.00	38.00		38.00	
	k				300.00	235.00	280.00		750.00	
	n				0.54	1.1	0.65		0.24	
	Rf				0.80	0.9	0.93		0.87	
	E	2000	45	45				5		
	u	0.35	0.45	0.45	0.40	0.40	0.30	0.30	0.30	10
	ϕ		8.00	14.00	11.00	38.00	35.00		35.00	0.30
2	c				32.00	0.00	38.00		38.00	
	k				300.00	235.00	280.00		750.00	
	n				0.54	1.10	0.65		0.24	
	Rf				0.80	0.90	0.93		0.87	
	E	2000	45	45				5		10
	u	0.35	0.45	0.40	0.40	0.40	0.30	0.30	0.30	0.30
	ϕ		7.50	11.00	11.00	38.00	35.00		35.00	
3	c				32.00	0.00	38.00		38.00	
	k				300.00	400.00	280.00		750.00	
	n				0.54	0.50	0.65		0.24	
	Rf				0.80	0.90	0.93		0.87	
	E	2000	45	45				5		10
	u	0.35	0.45	0.40	0.40	0.40	0.30	0.30	0.30	0.30
	ϕ		7.50	11.00	11.00	38.00	35.00		35.00	
4	c				32.00	0.00	38.00		38.00	
	k				300.00	400.00	280.00		750.00	
	n				0.54	0.50	0.65		0.24	
	Rf				0.80	0.90	0.93		0.87	

	E	2000	45	45				5		10
	u	0.35	0.45	0.40	0.40	0.40	0.30	0.30	0.30	0.30
	ϕ		8.00	14.00	38.00	37.00	35.00		35.00	
5	c				32.00	0.00	38.00		38.00	
	k				750.00	400.00	280.00		750.00	
	n				0.24	0.24	0.65		0.24	
	Rf				0.80	0.90	0.93		0.87	

E - Elastic Modulus (Mpa)
u - Poisson's Ratio
ϕ - Friction Angle (degree)
c - Cohesion (Kpa)
k - Modulus number for hyp. model
Rf - Failure ratio for the hyp. model
Unit weights same as Table 2

Ts1 - Tailing sand using linear elastic model when layer is added
Ts2 - Tailing sand using linear elastic model
Ts3 - Tailing sand using linear elastic model to miminize convergence problem at the toe of the dyke

Table 4: Summary of the material parameters used in the non-linear effective stress analyses

List of Figures

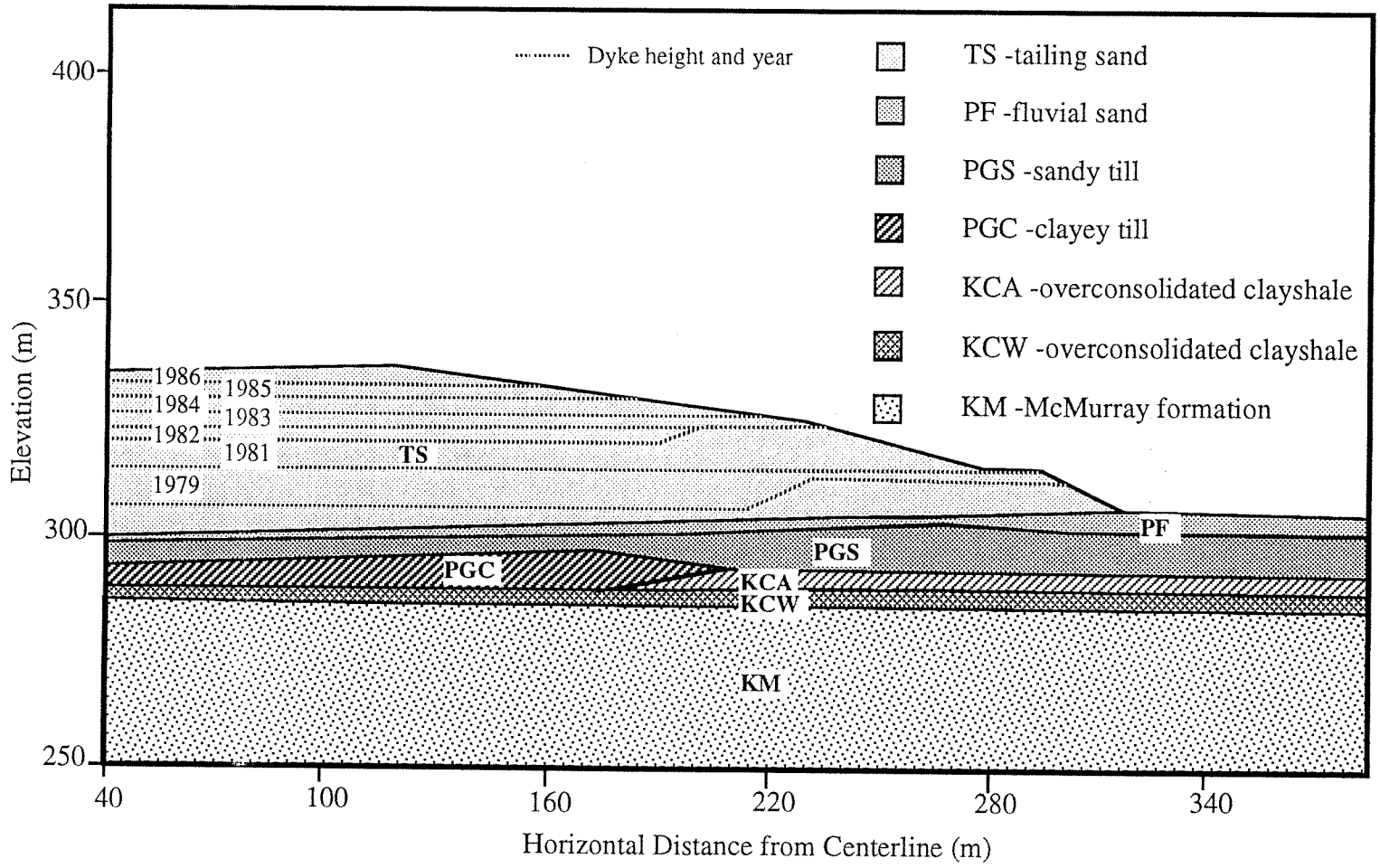

Figure 1: Stratigraphy of Cell 23, Section 53, in 1986.

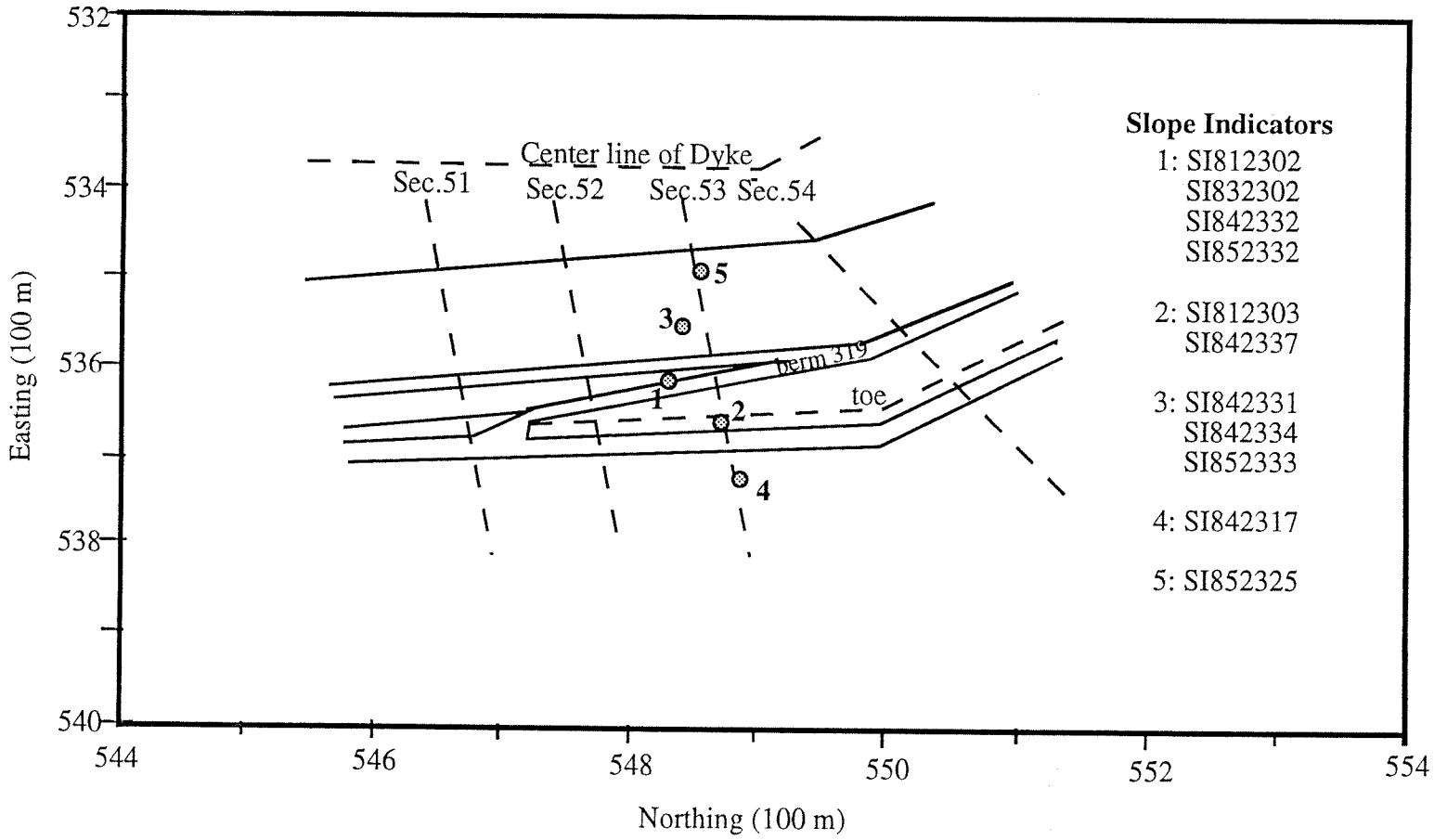

Figure 2: Plan view of slope indicators locations.

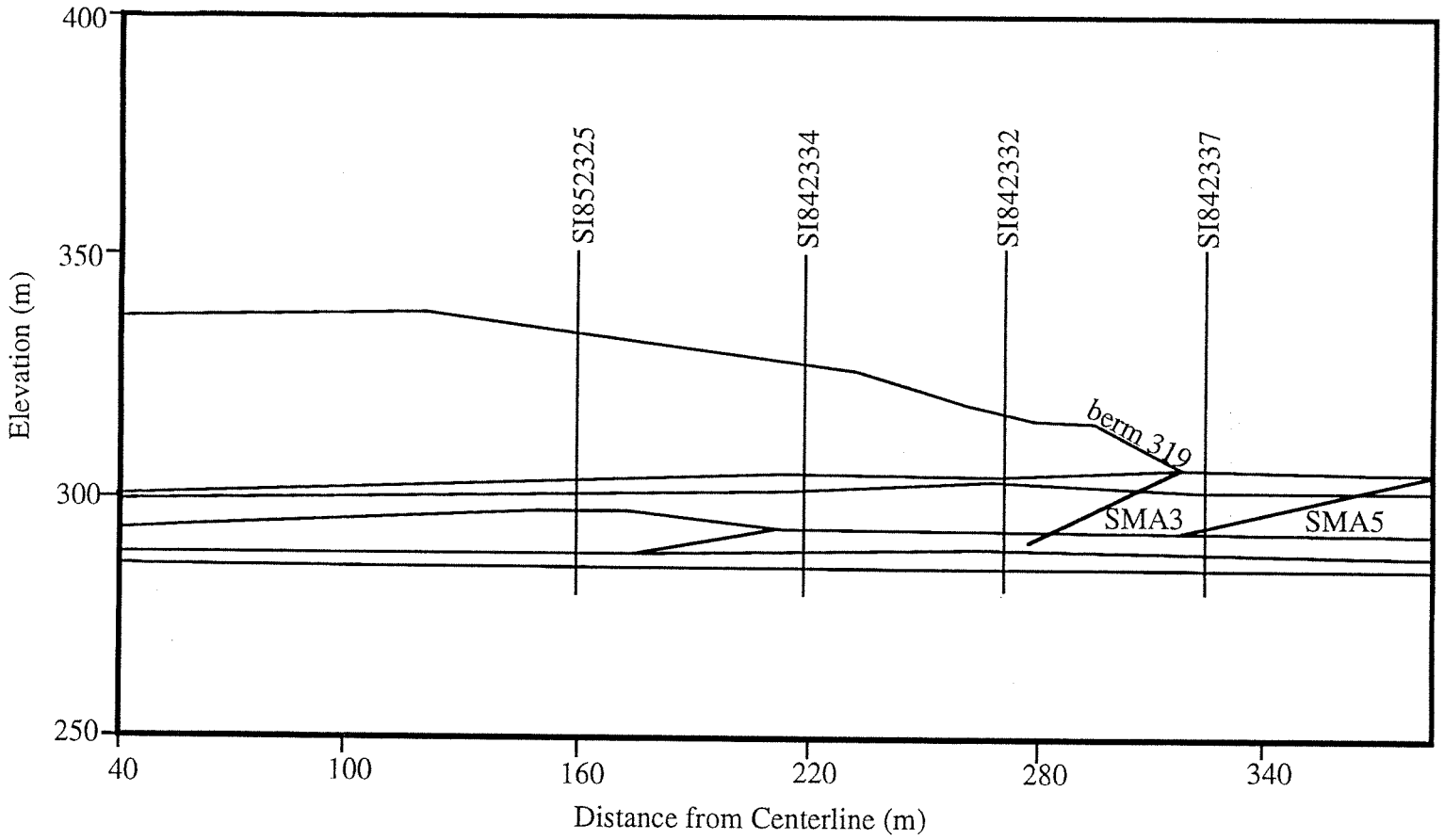

Figure 3: Cross section of dyke showing slope indicators locations.

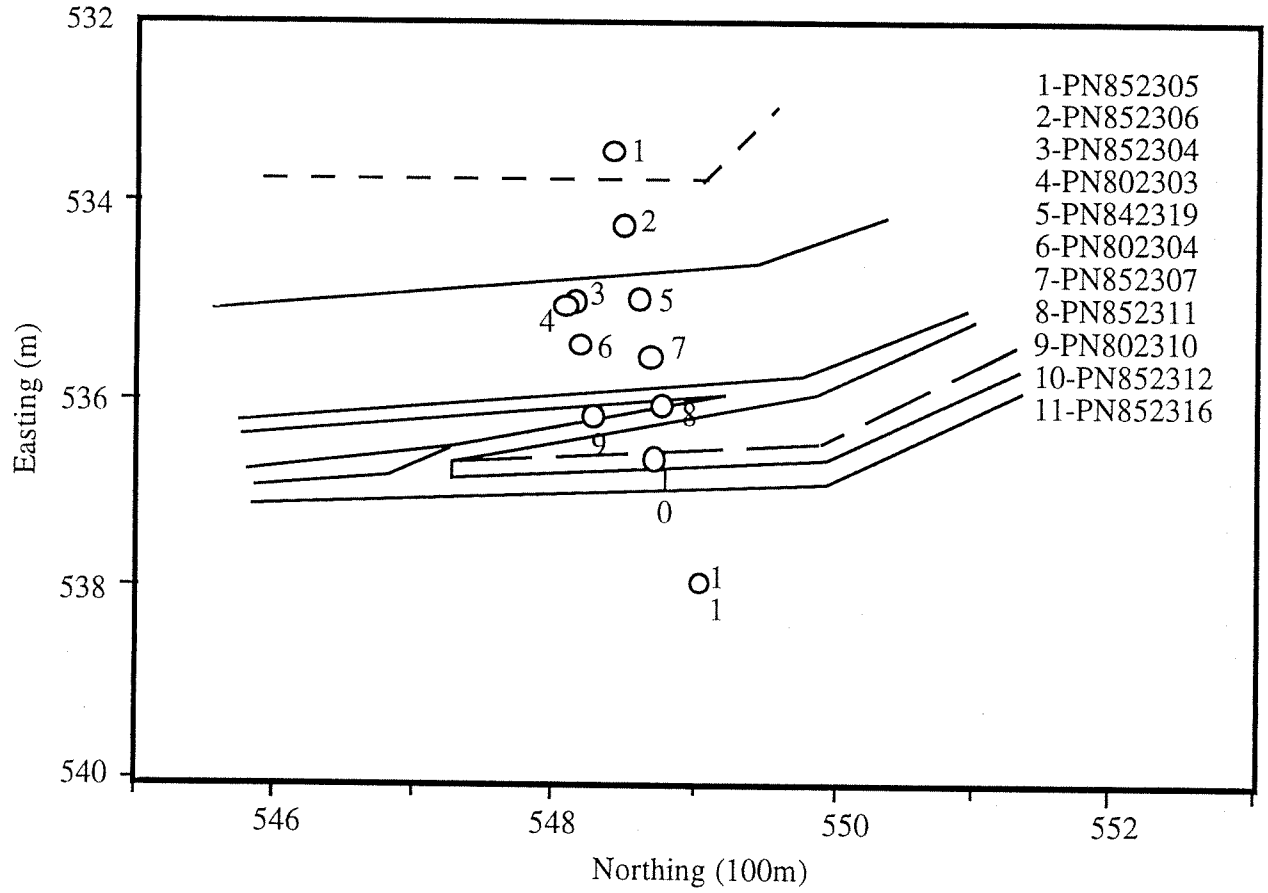

Figure 4: Plan view of dyke indicating piezometers locations.

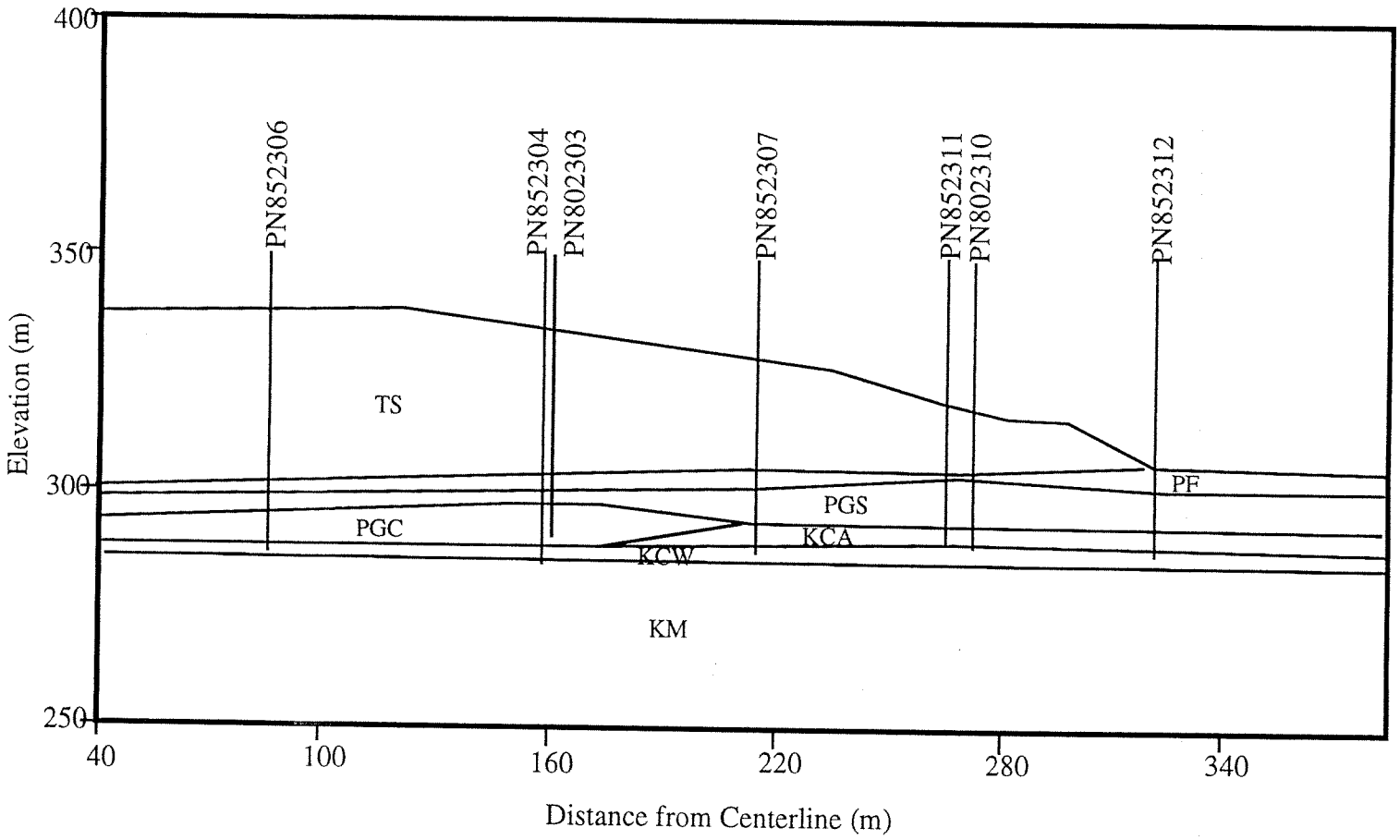

Figure 5: Cross section of dyke showing piezometers locations.

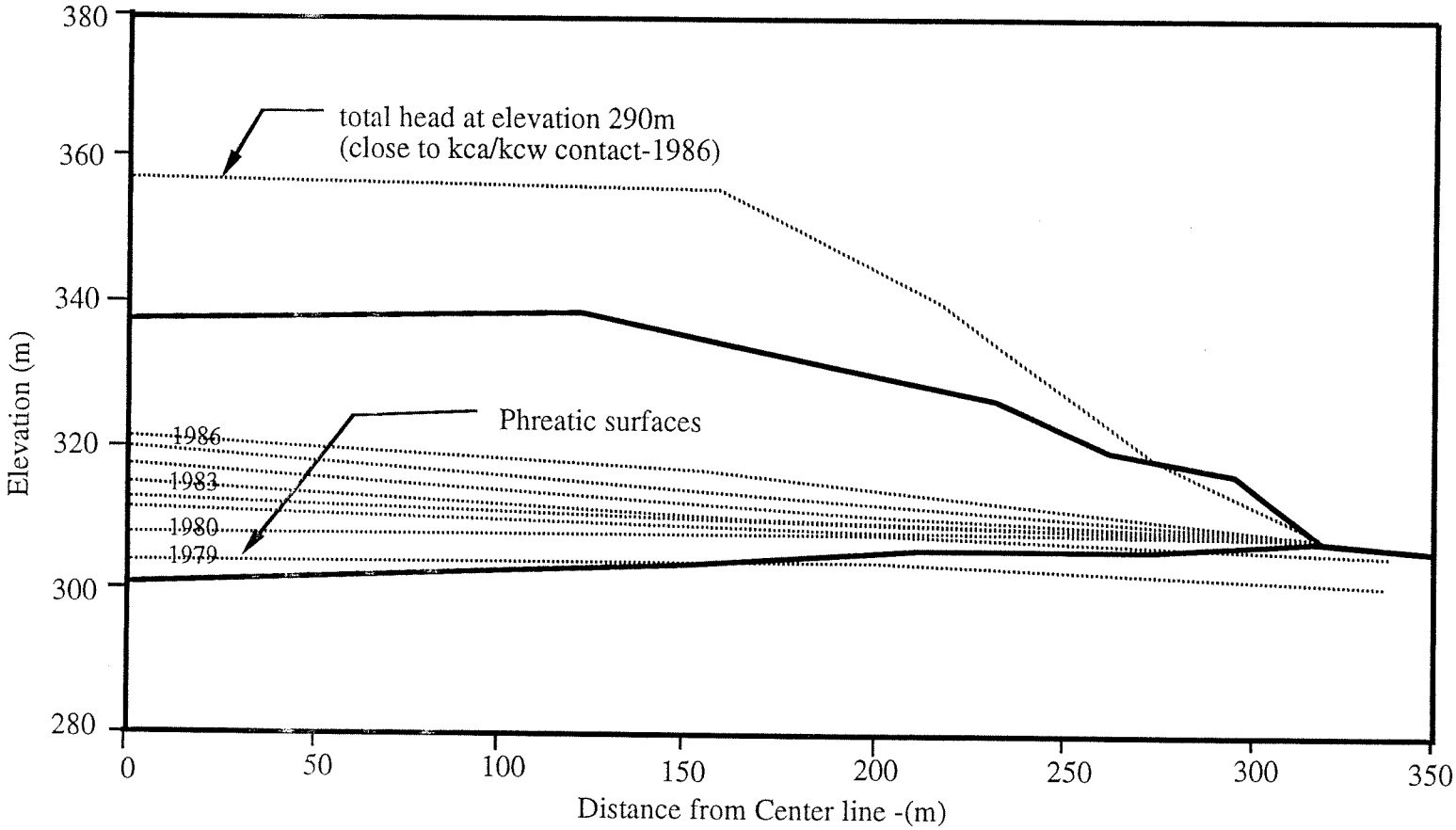

Figure 6: Phreatic surface at each year of construction and average total head at elevation 290 m measured in 1986.

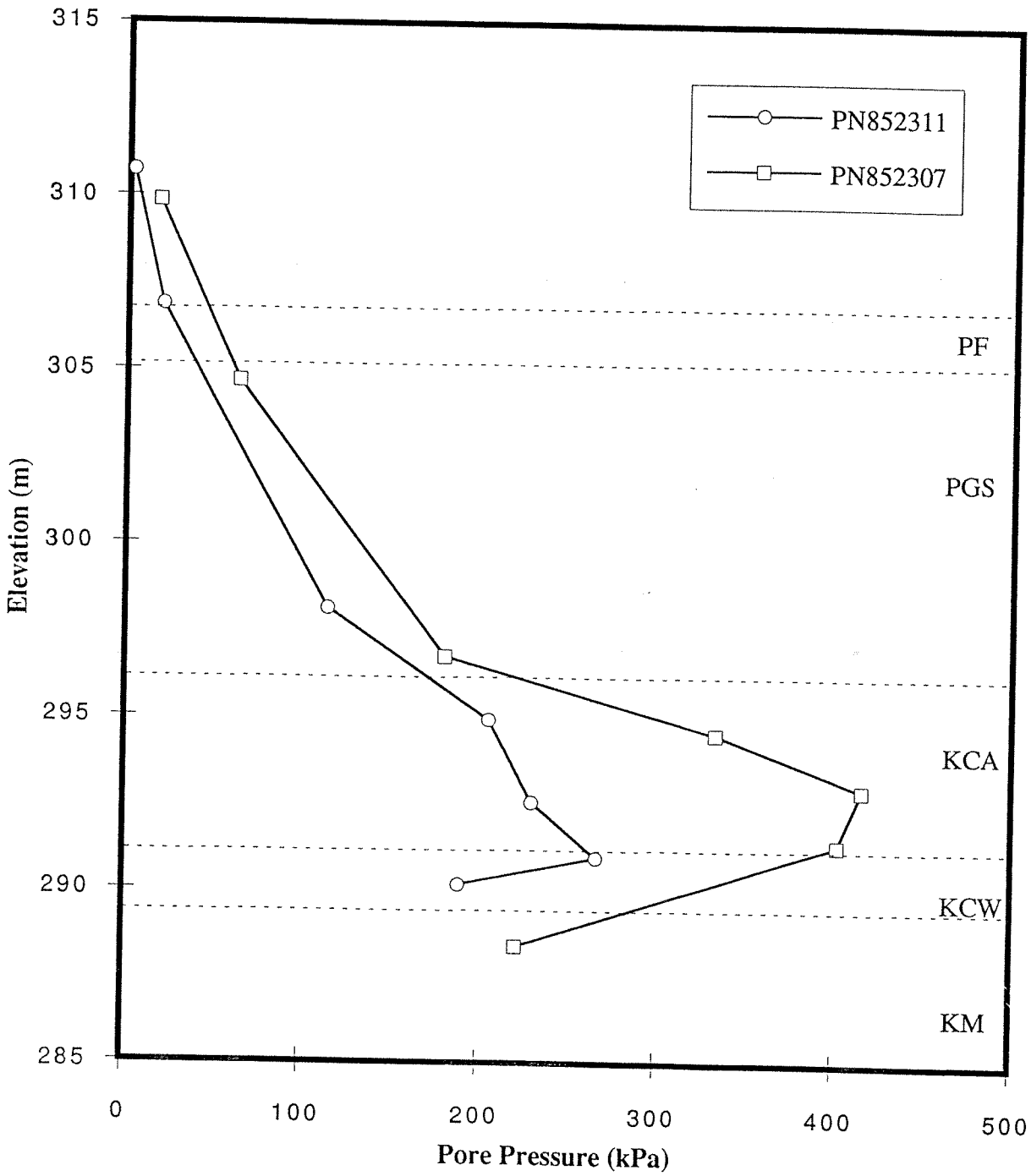

Figure 7: Average pore pressure measured by PN852307 and PN852311 in 1985.

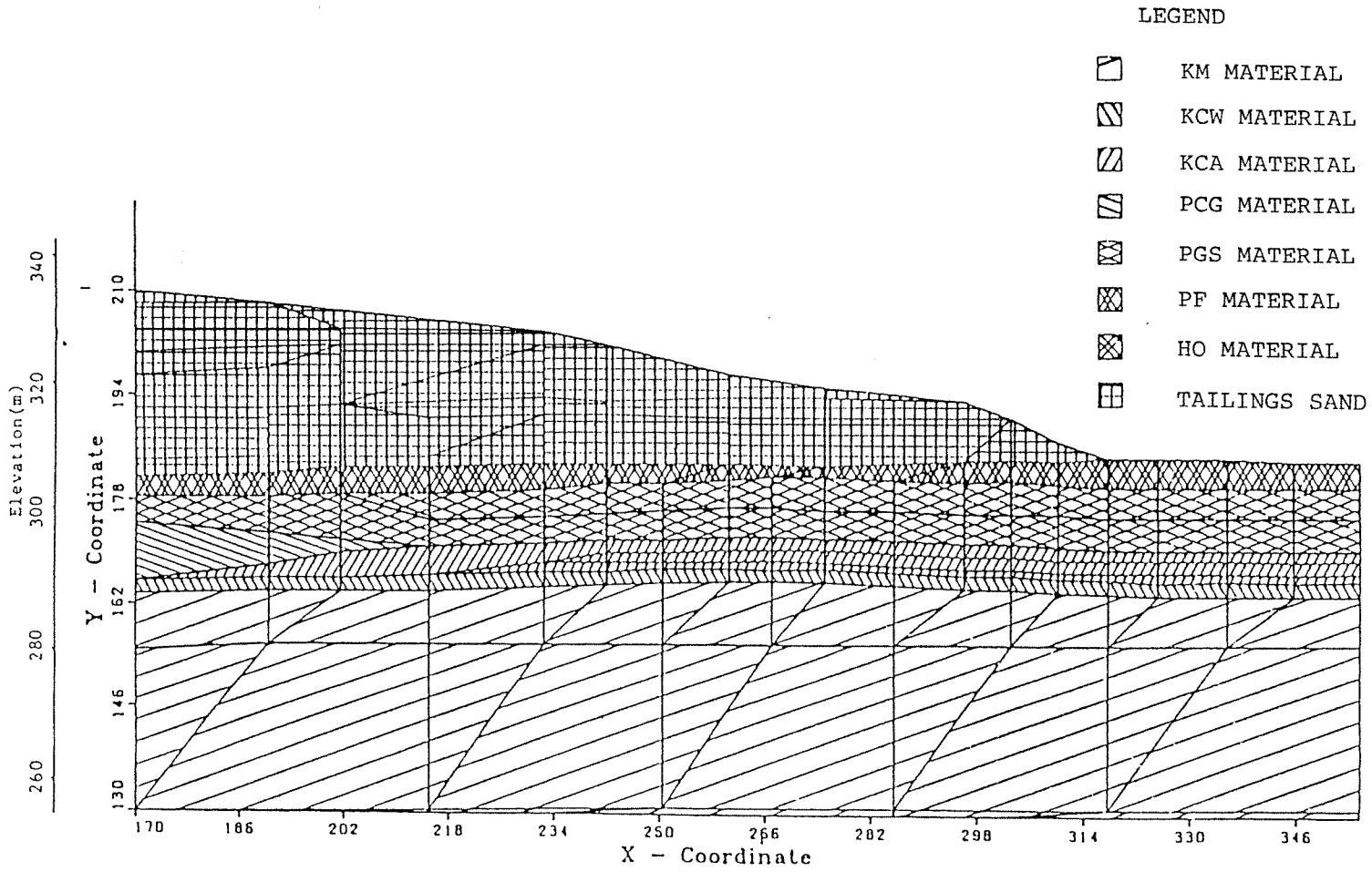

Figure 8: Soil stratigraphy used in the finite element analyses.

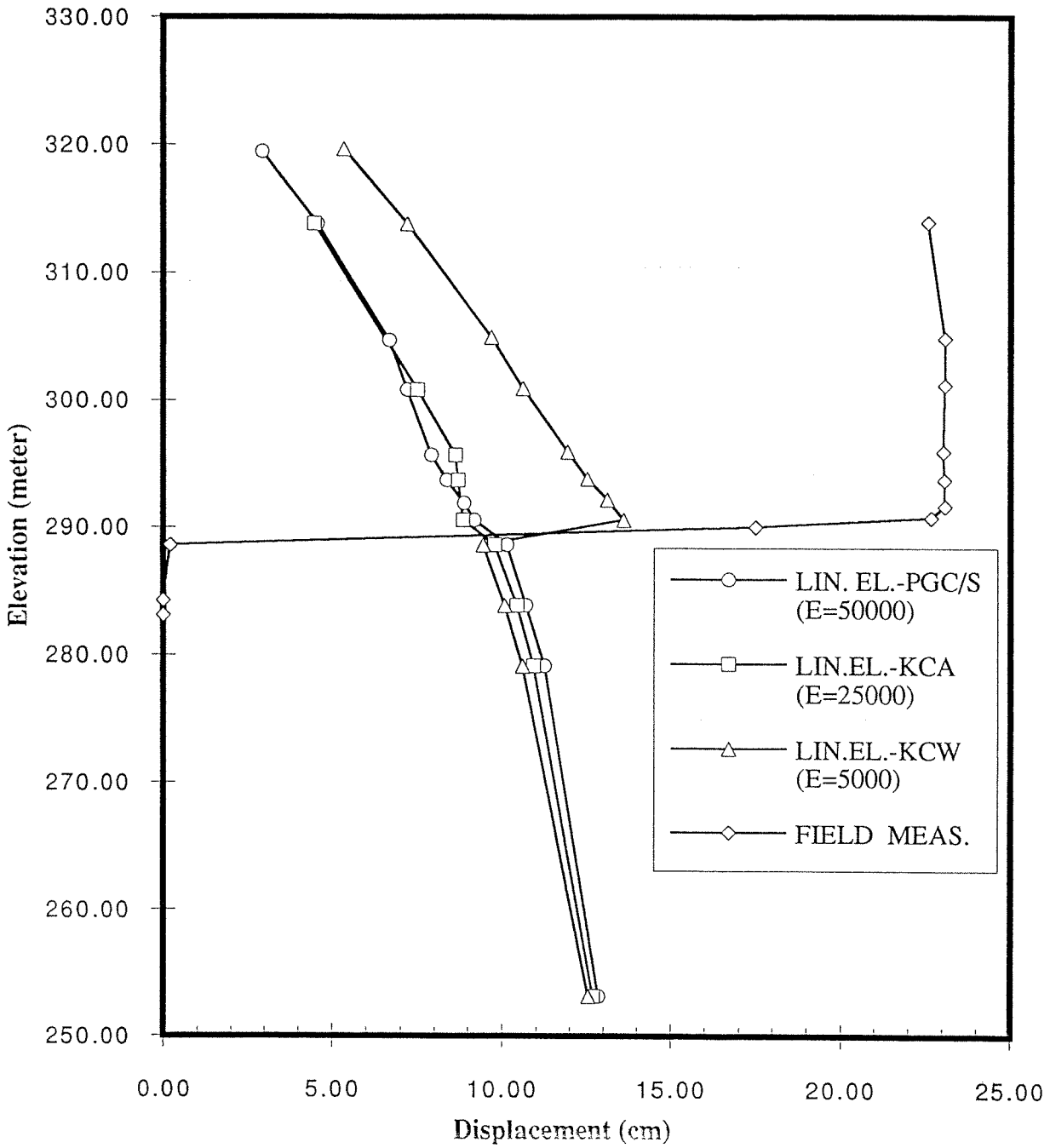

Figure 9: Comparison between measured and calculated horizontal displacements at SI842332(Berm 319) position for reduced modules for KCW material - linear elastic analysis.

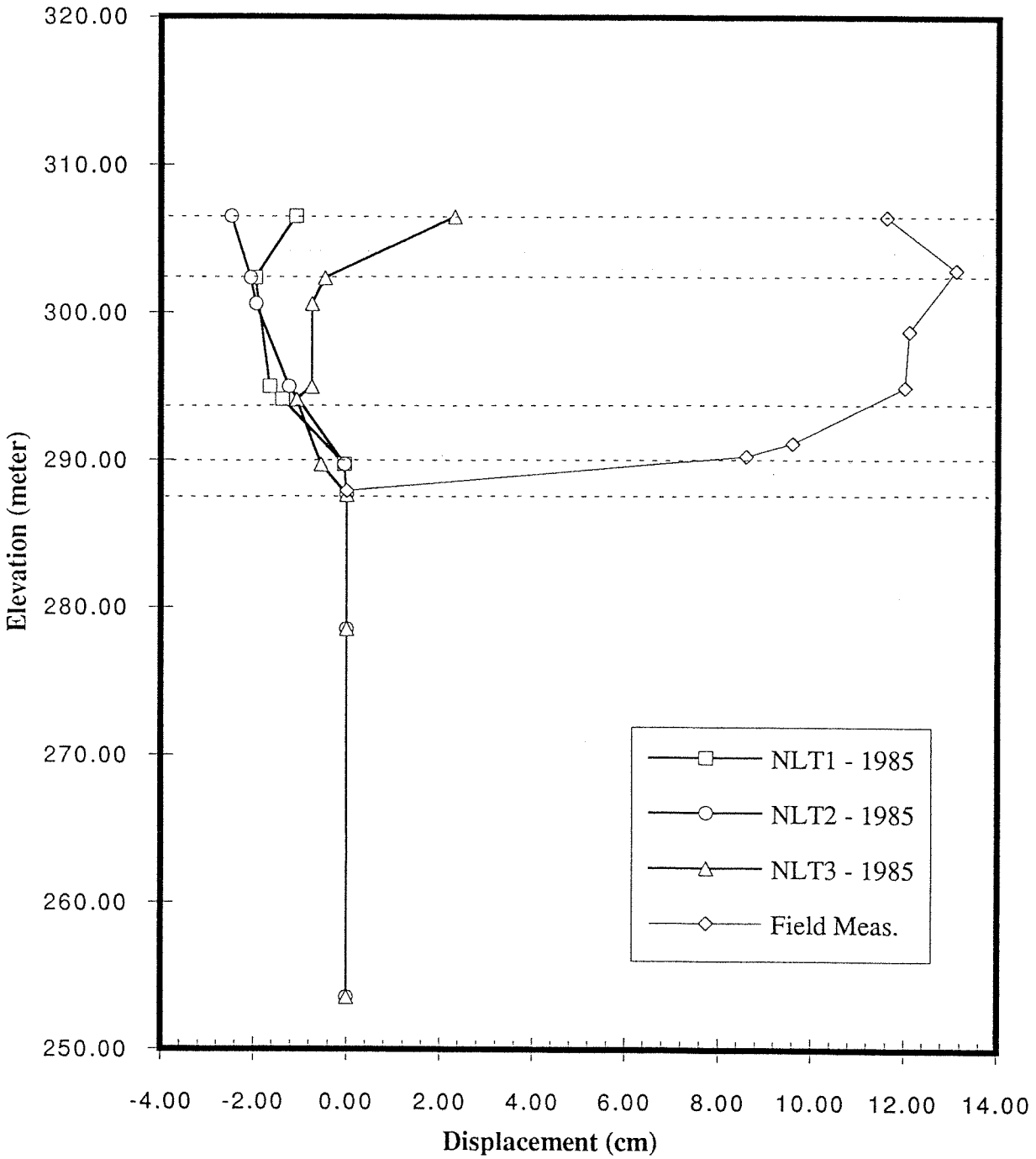

Figure 10: Comparison between measured and calculated horizontal displacements at SI8423342(crest) position for non-linear total stress analysis.

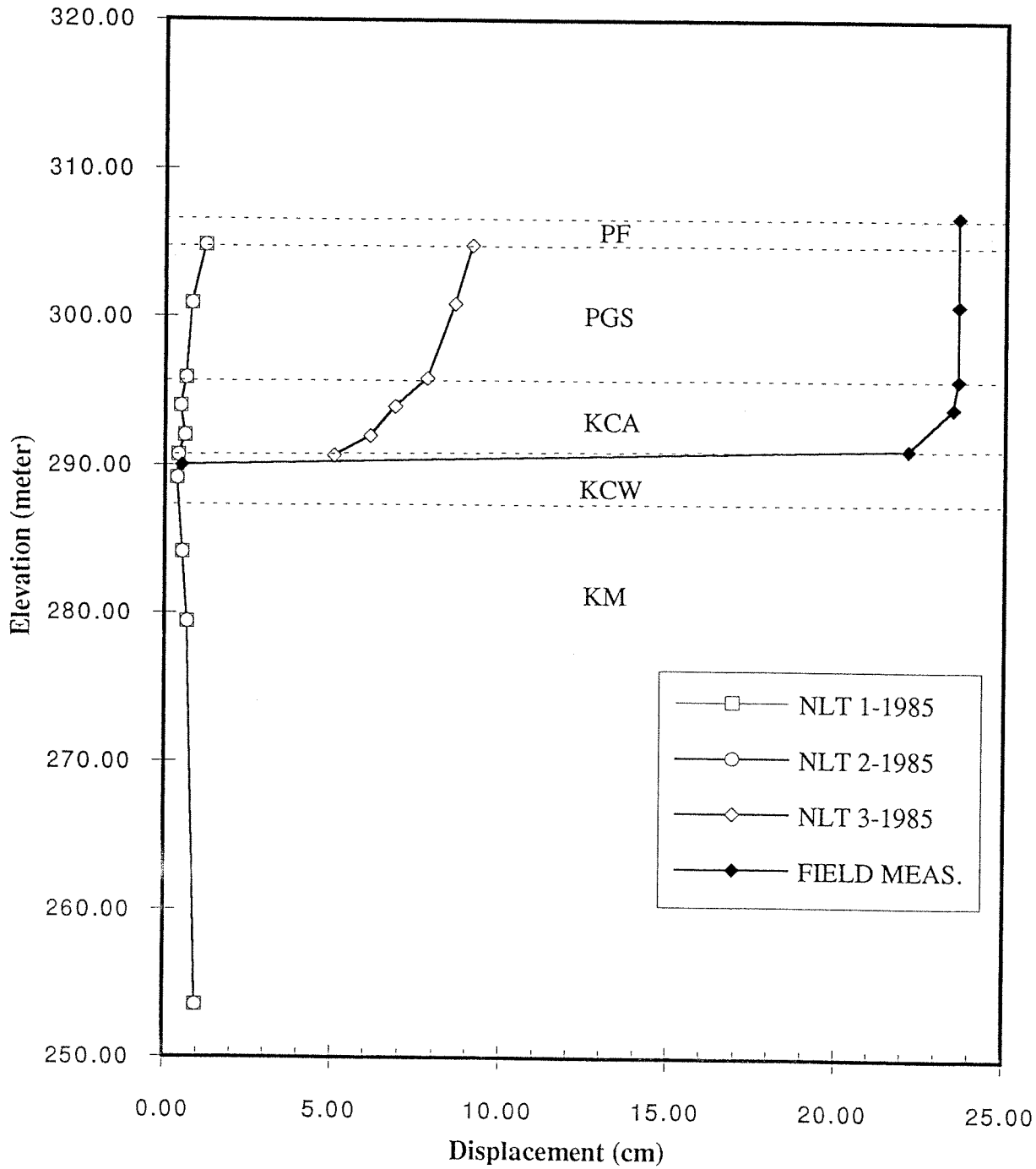

Figure 11: Comparison between measured and calculated horizontal displacements at SI842332(berm 319) position - nonlinear total stress analysis.

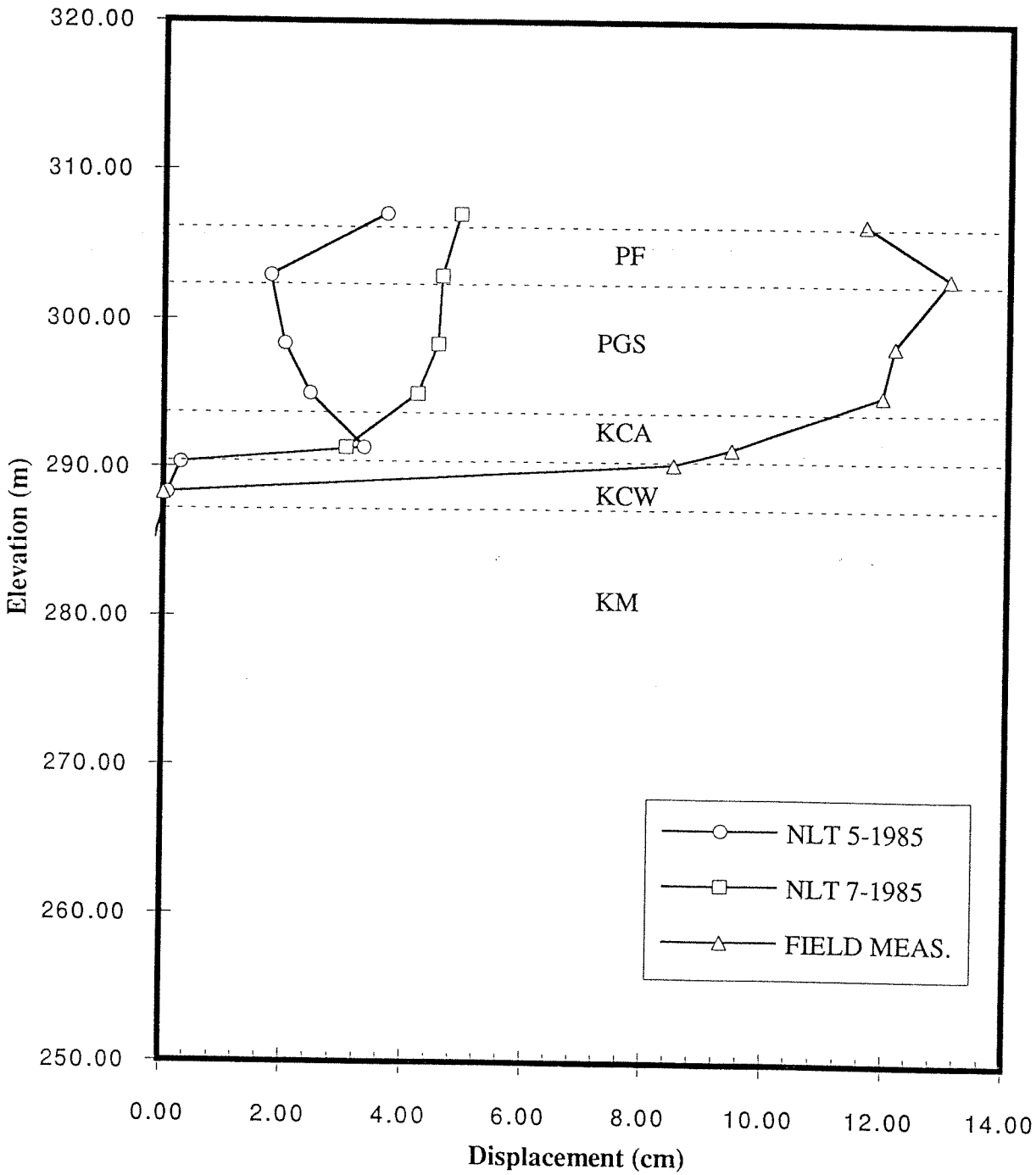

Figure 12: Comparison between measured and calculated horizontal displacements at SI842334(crest) position - nonlinear total stress analysis.

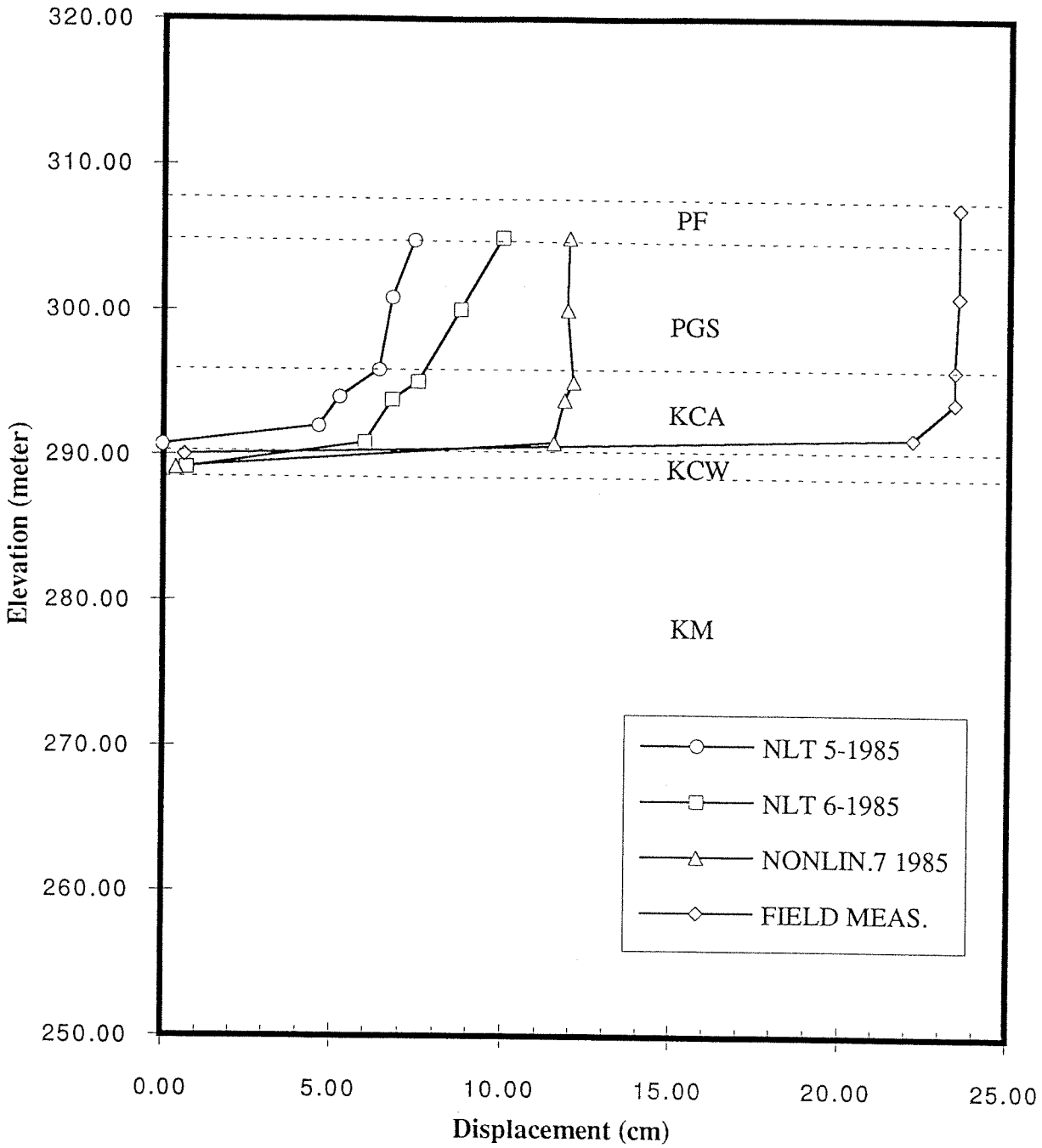

Figure 13: Comparison between measured and calculated horizontal displacements at SI842332(berm 319) position - nonlinear total stress analysis.

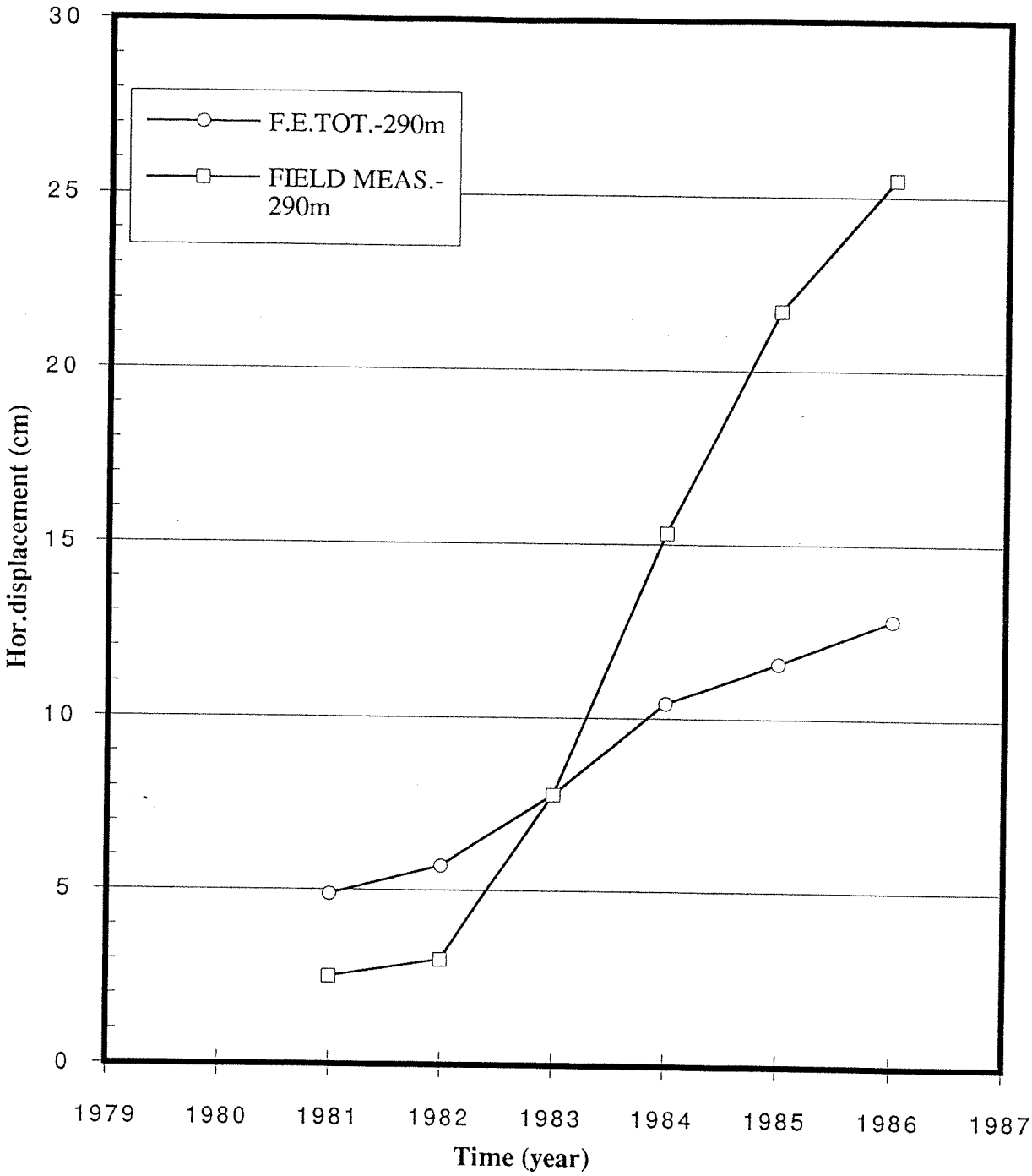

Figure 14: Comparison between measured and calculated horizontal displacements with time at SI842332(berm 319) position (elevation 290m) - nonlinear total stress analysis.

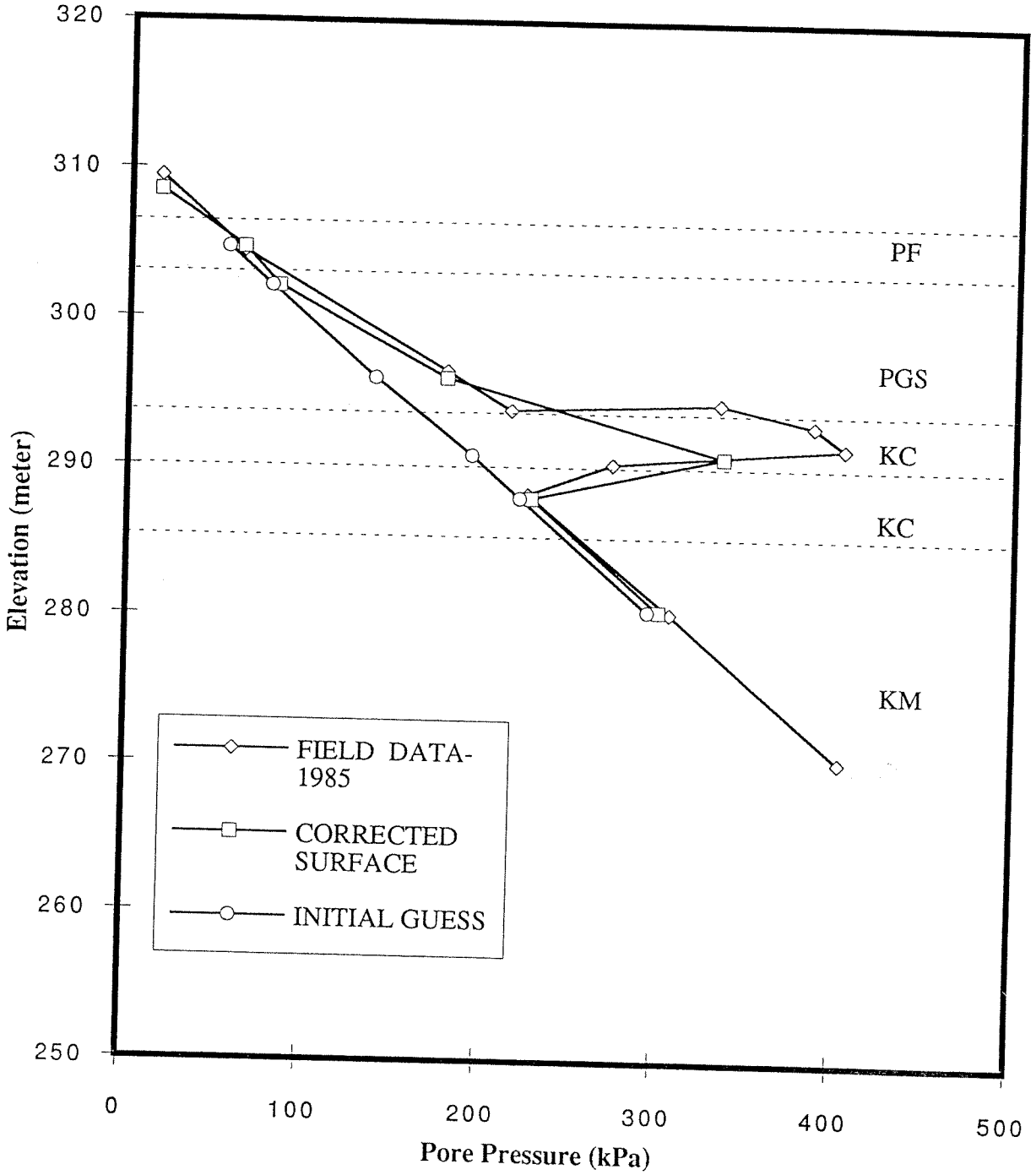

Figure 15: Comparison between measured and interpolated pore pressures at PN852307 position.

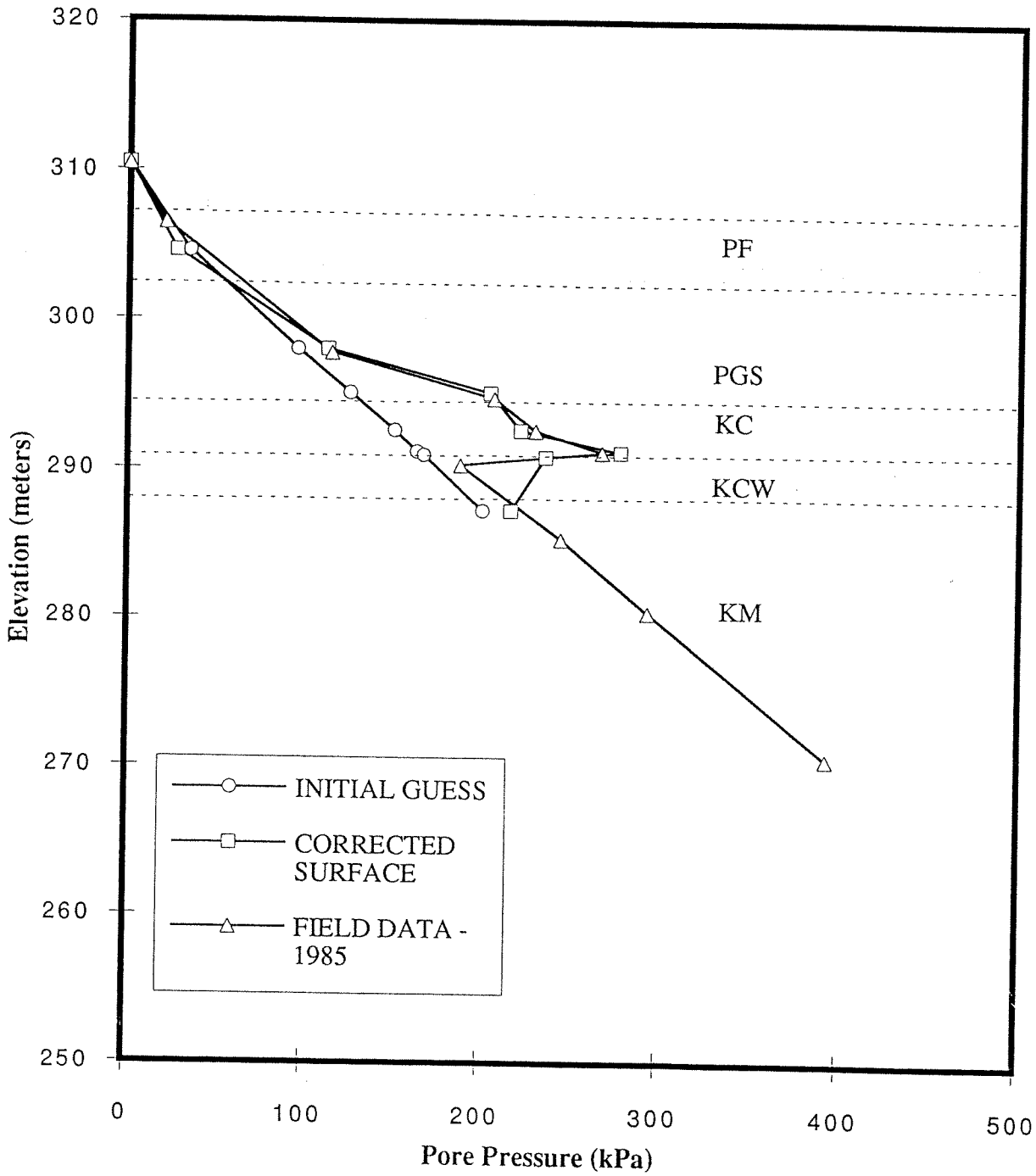

Figure 16: Comparison between measured and interpolated pore pressure at PN852311 position.

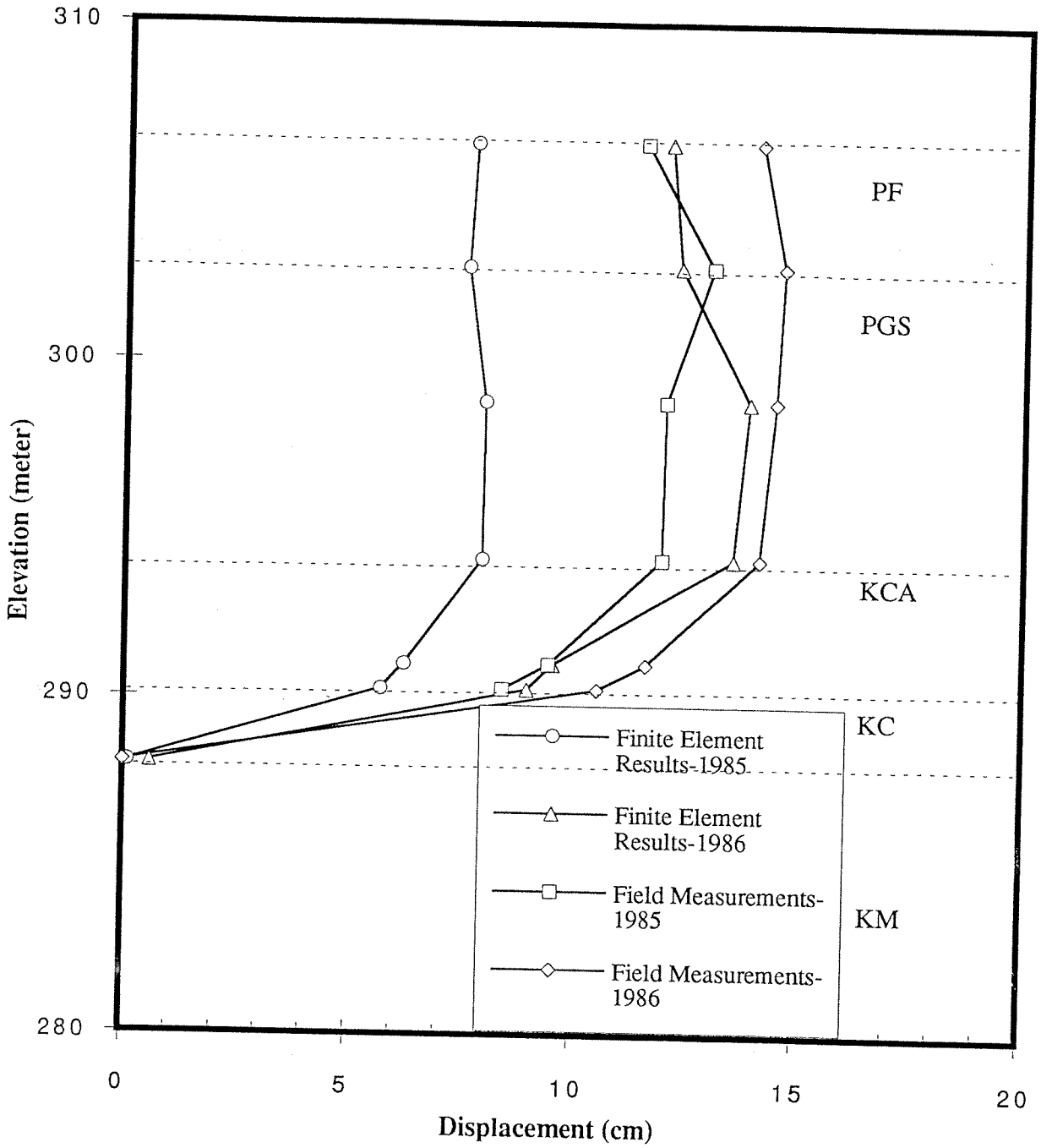

Figure 17: Comparison between measured and calculated horizontal displacements at SI842334(crest) position - nonlinear effective stress analysis.

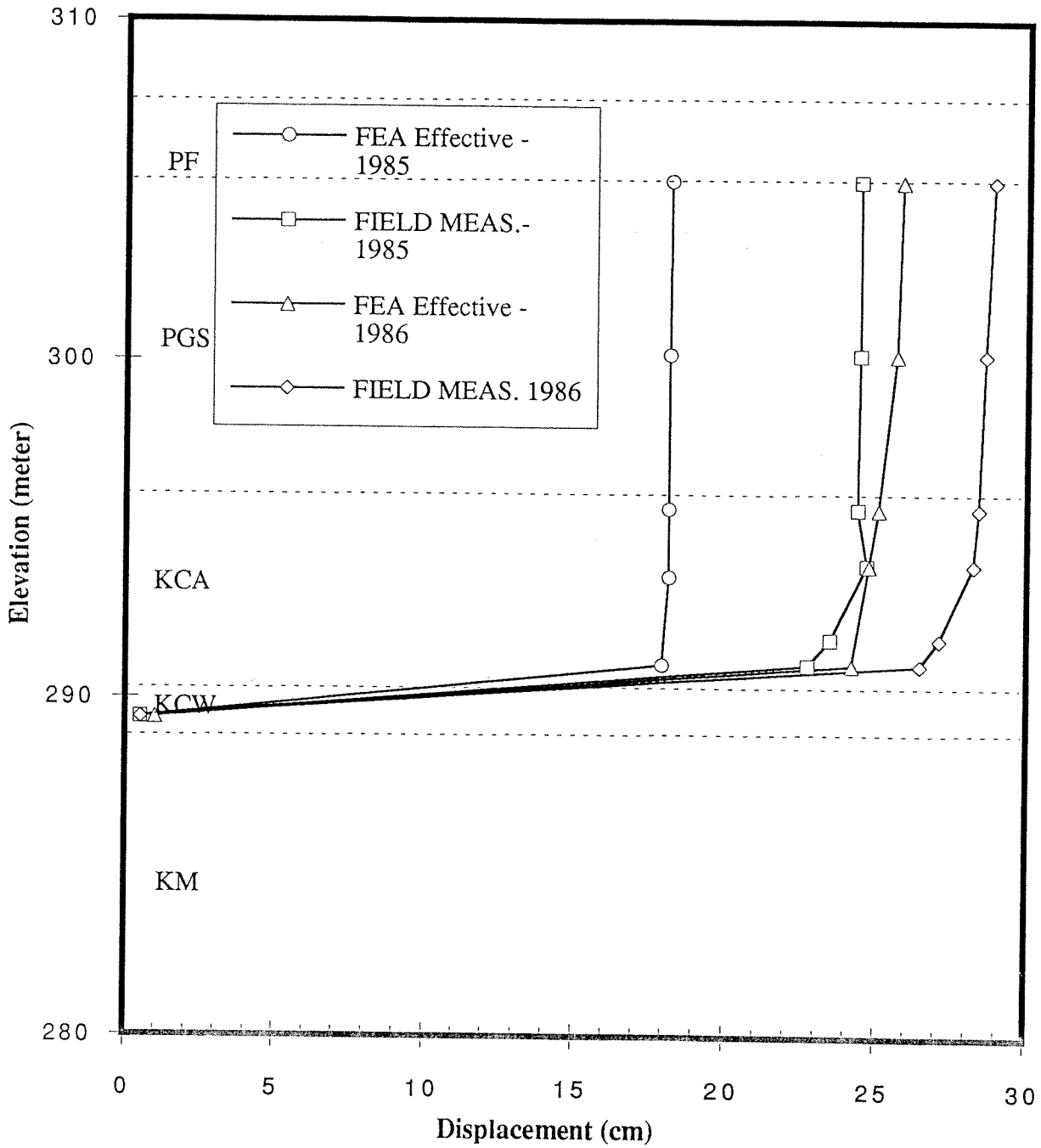

Figure 18: Comparison between measured and calculated horizontal displacements at SI842332(berm 319) position - nonlinear effective stress analysis.

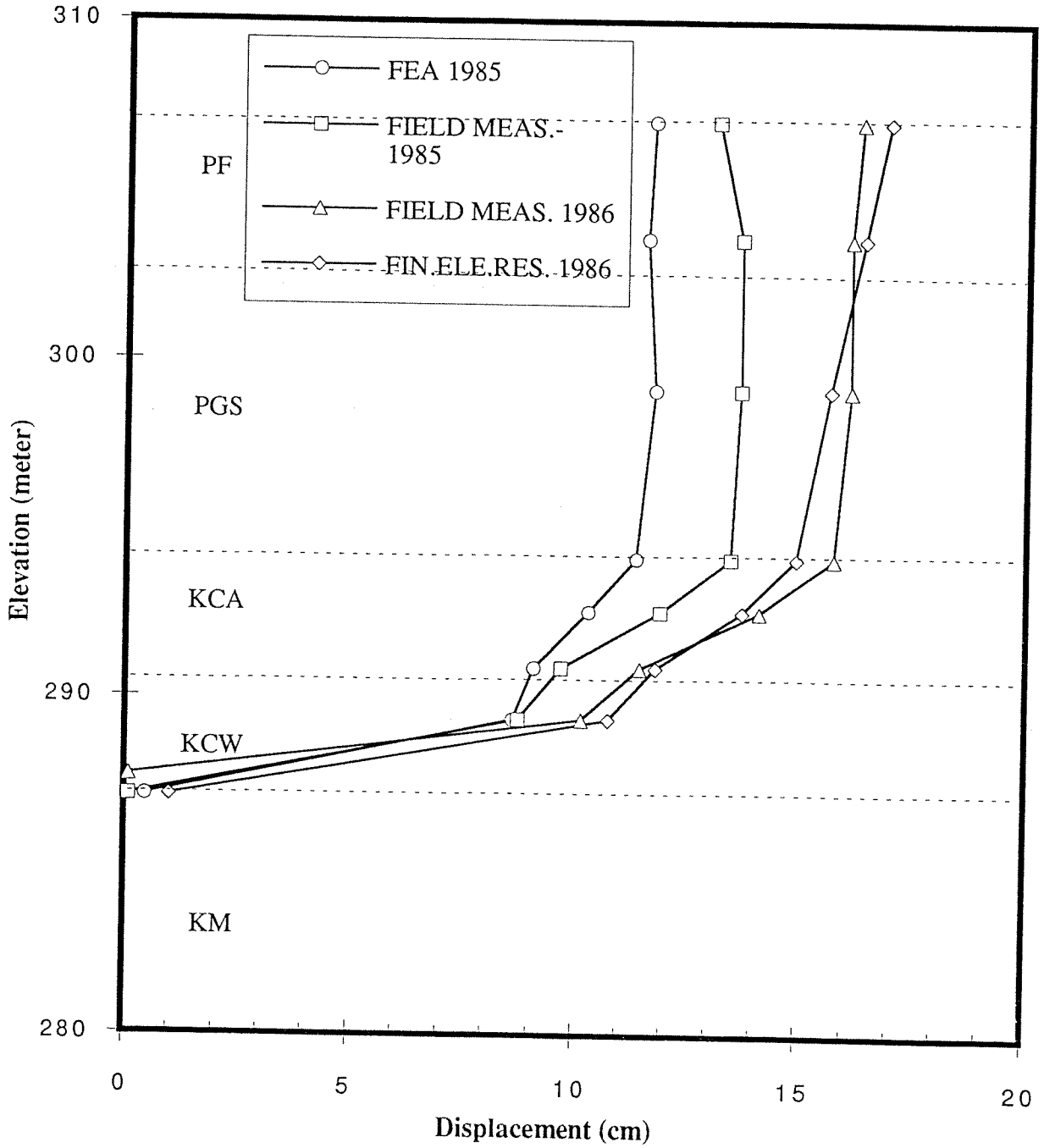

Figure 19: Comparison between measured and calculated horizontal displacements at SI842337(toe) position - nonlinear effective stress analysis.

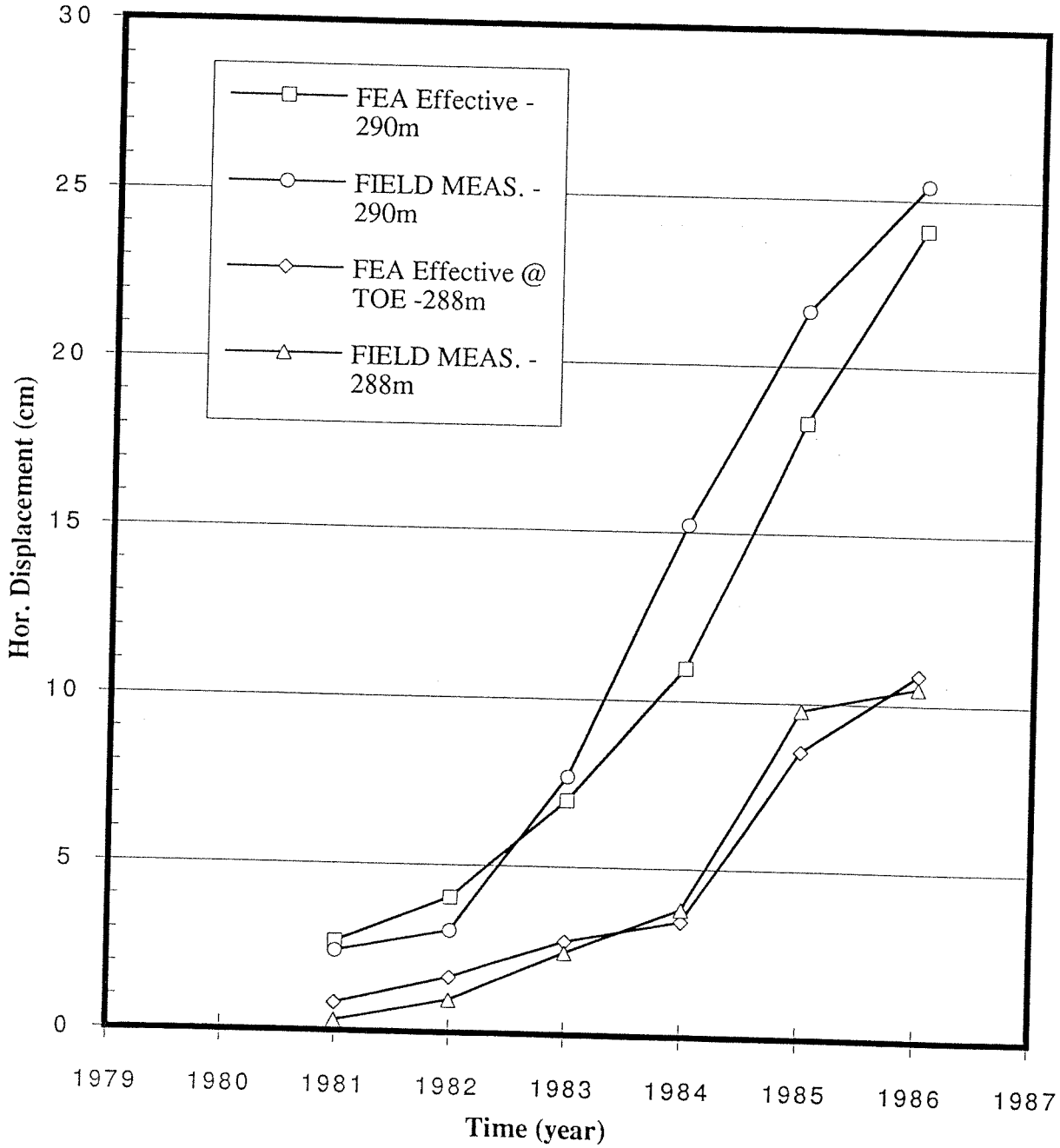

Figure 20: Comparison between measured and calculated horizontal displacements with time at SI842332(berm 319) and SI842337(toe) positions at elevation of KCA/KCW contact - nonlinear effective analysis.

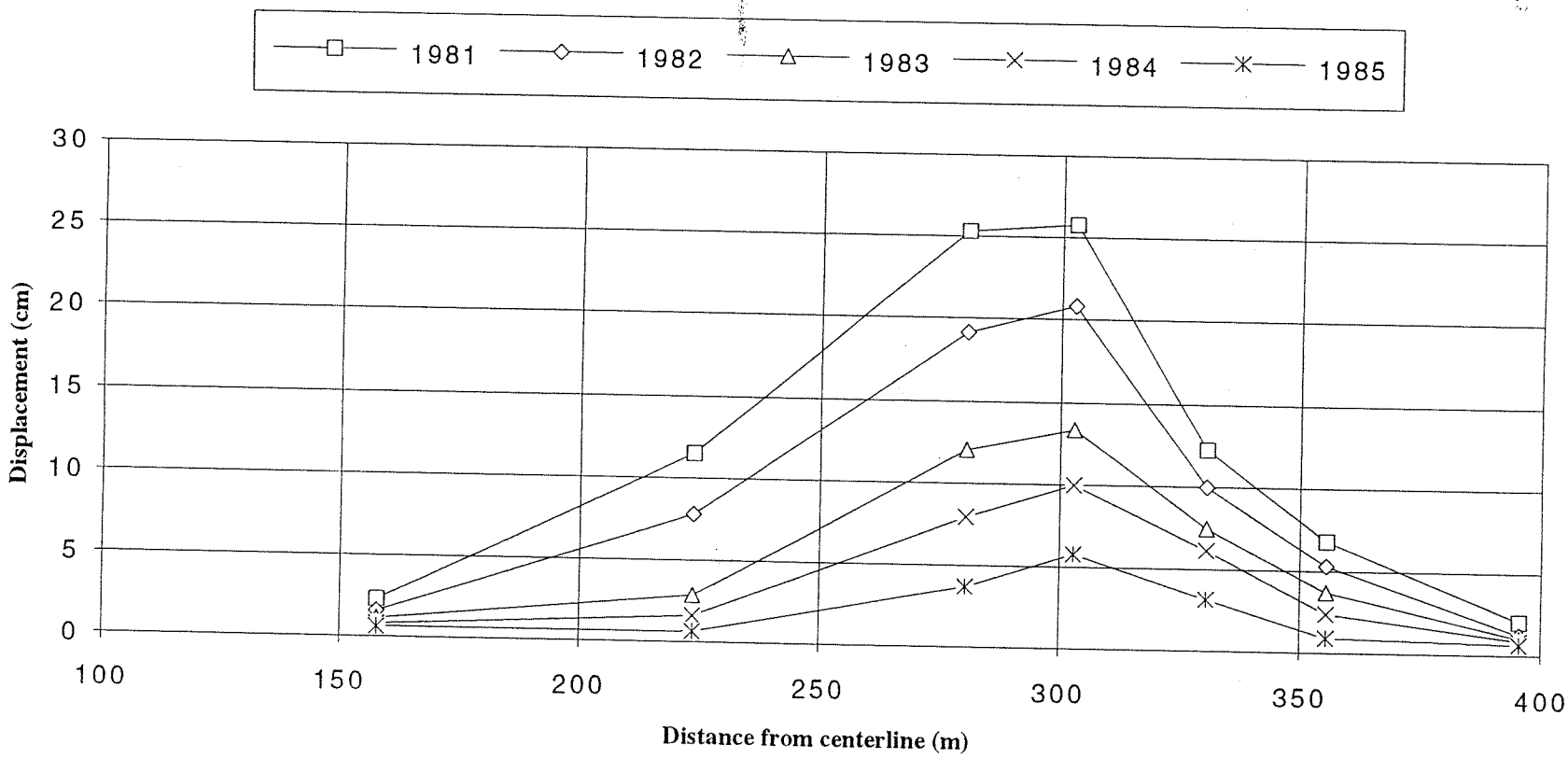

Figure 21: Calculated horizontal displacements along KCA/KCW contact - nonlinear effective stress analysis.

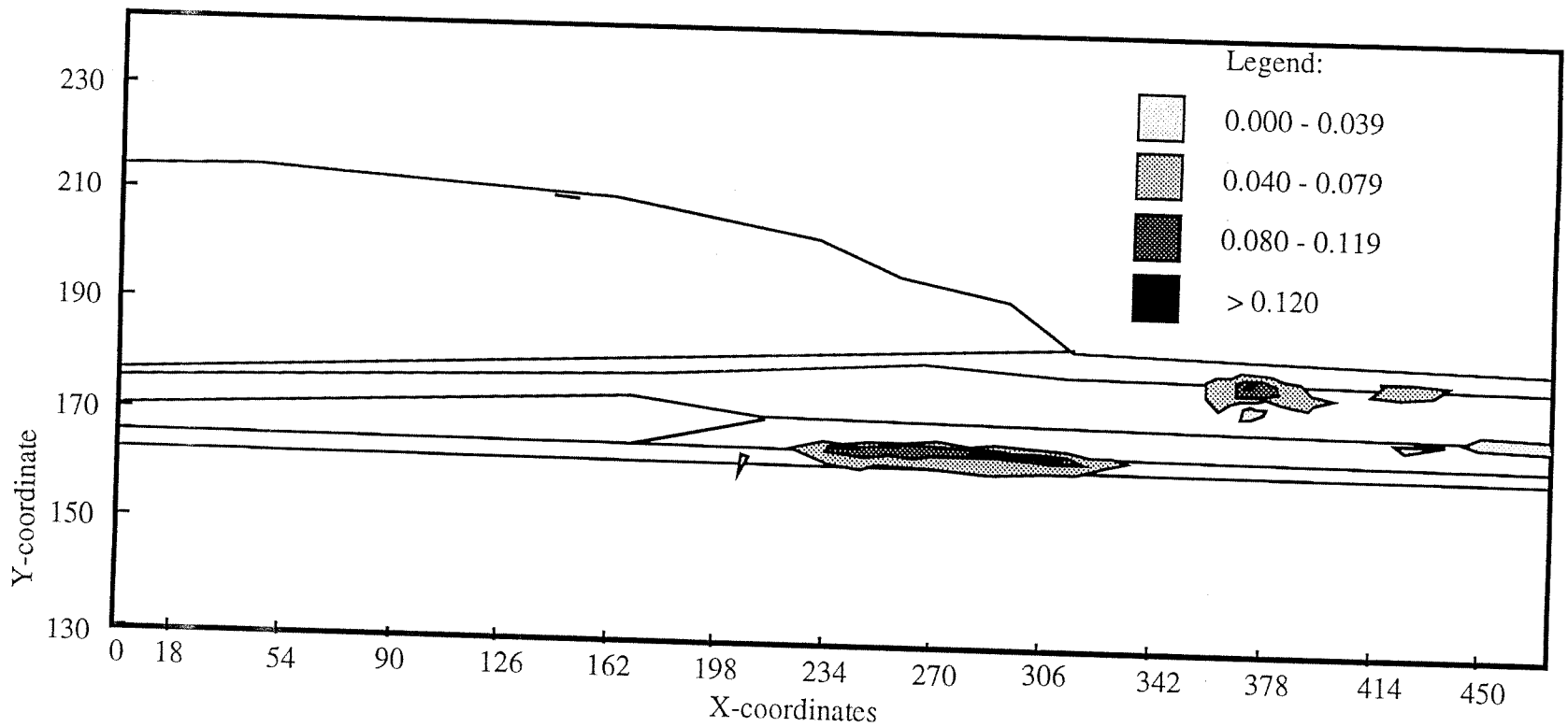

Figure 22: Contours of maximum shear strain - 1986.

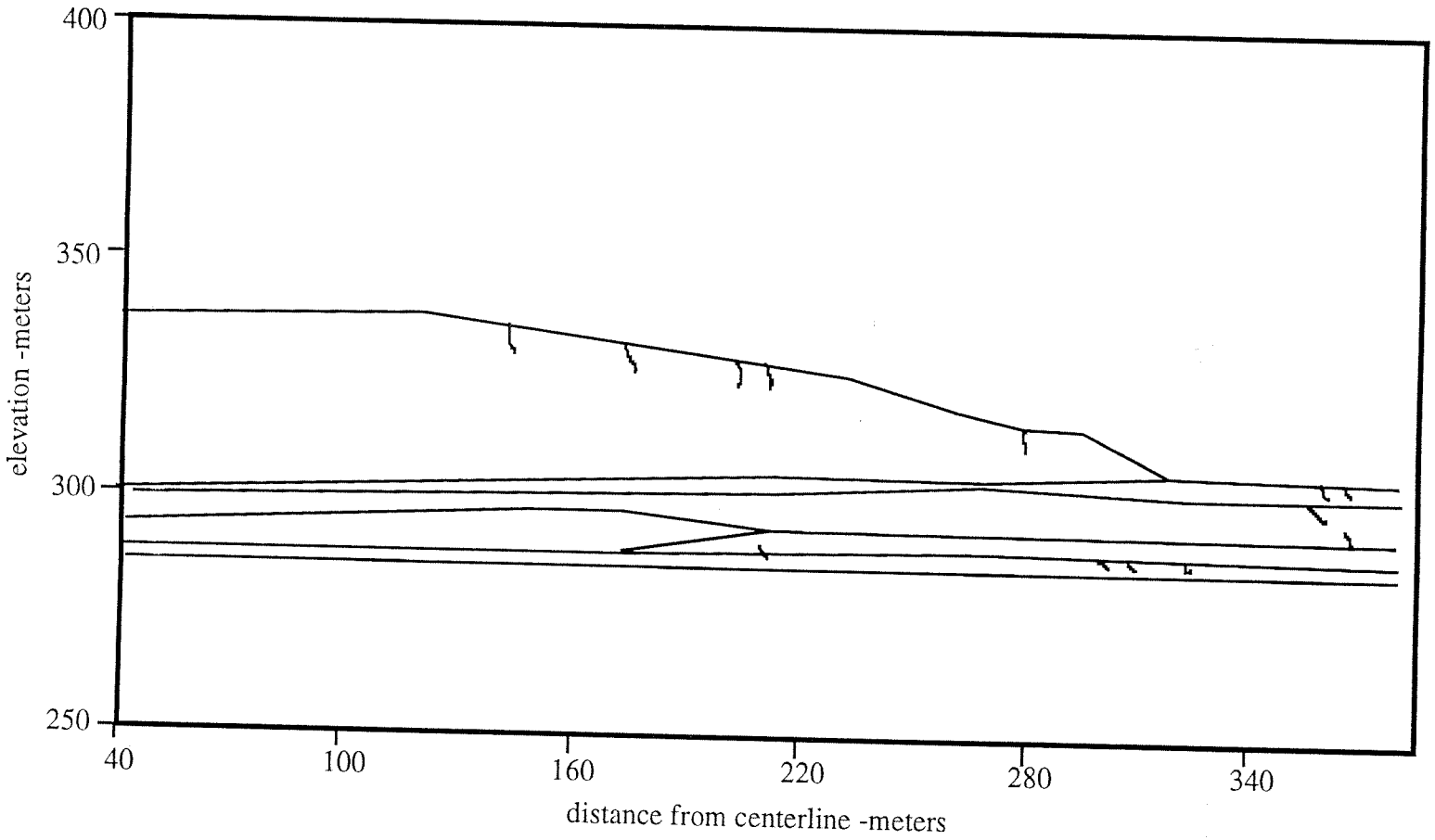

Figure 23: Schematic representation of the cracks - 1986.